REVIEW PAPER

Plasma-based synthesis of graphene and applications: a focused review

Muhammad Adeel Zafar[1] · **Mohan V. Jacob**[1]

Abstract

Graphene is a highly sought-after material for a wide range of applications, particularly in areas such as energy harvesting and storage, electronics, electrochemical sensors, biomedical, composites, and coatings. The synthesis of high-quality graphene is a precondition for its real-time application. However, conventional synthesis methods have certain drawbacks including laborious procedures and structural defects in graphene nanosheets. Plasma-based synthesis techniques such as plasma-enhanced chemical vapor deposition and atmospheric pressure microwave plasma are high-tech synthesis practices that can produce graphene without any solvents in a few seconds. This article reviews these state-of-the-art techniques emphasizing mainly their process parameters for the synthesis of high-grade graphene, which is defect-free, and comprises mono to few layers, great carrier mobility, and high purity. The applications of as-synthesized graphene in various fields are also provided. Moreover, the potential breakthroughs and the prospect of these techniques are also discussed in this work.

Keywords Plasma-enhanced chemical vapor deposition · Atmospheric pressure microwave plasma · Process parameters · Growth of graphene

1 Introduction

The astonishing discovery in the field of materials science in the last two decades is indeed graphene. Graphene was synthesized by Professor Andre Geim and Konstantin Novoselov in 2004 who won a noble prize for this (Hancock 2011). Although graphene was under investigation before 2004 under different names, however, due to the lack of suitable synthesis techniques, graphene failed to appear in the limelight. Prof. Geim and Novoselov used a simple approach of mechanical exfoliation,

✉ Mohan V. Jacob
mohan.jacob@jcu.edu.au

1 Electronics Materials Lab, College of Science and Engineering, James Cook University, Townsville, Queensland 4811, Australia

which involved using scotch tape on graphite (Allen et al. 2009). Eventually, the exfoliated single layer of graphite, comprising a thickness between 0.4 and 1.7 nm was termed graphene (Shearer et al. 2016).

Graphene is a 2-dimensional monolayer of carbon atoms arranged in a honeycomb structure. It is basically composed of sp^2 hybridized carbon atoms. Just like other allotropes of carbon i.e., diamond, graphite, fullerenes (C_{60}), and carbon nanotube, graphene is also an allotrope of carbon (Shunhong, et al. 2015). Graphene has a large theoretical specific area (Wei and Qu 2012) and possesses extraordinary mechanical, electrical, optical, thermal, etc. properties (Iqbal et al. 2020). It is the thinnest as well as the strongest known material, surpassing diamond (Wagner et al. 2017). Owing to all these properties, Prof. Geim called it a "wonder material" (Geim and Graphene 2009). Also referred to as "magic material" in some writings by others (Aliofkhazraei 2013).

The main challenge towards the practical application of any material comes during its synthesis process. A variety of synthesis techniques have been used to produce pristine graphene. Mainly, it can be divided into bottom-up and top-down approaches, which are further divided into various techniques based on the synthesis approach. Each synthesis method has its own merits and demerits (Bhuyan et al. 2016). Figure 1 gives the division of techniques.

The methods which involve the breakdown of the bulk material, such as graphite to acquire a single or few layers of graphene are regarded as top-down methods. Based on how exfoliation is carried out, various techniques have been reported as top-down methods. It includes, mechanical exfoliation (Park et al. 2010), Chemical synthesis, liquid-phase exfoliation (Lee et al. 2017) etc. However, these techniques lack a good production rate, give poor quality of graphene (Whitener and Sheehan 2014), or require the reaction of graphite with strong oxidizers such as sulphuric
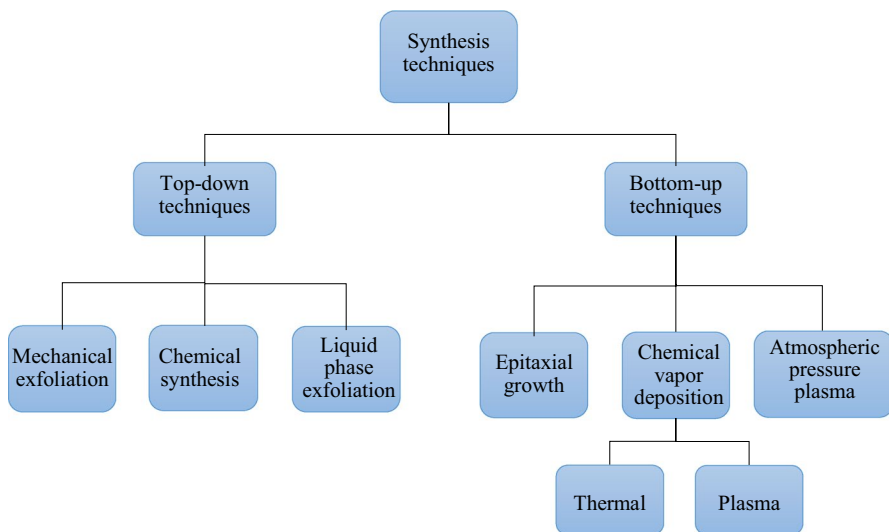
Fig. 1 Top-down and bottom-up synthesis techniques of graphene

acid, potassium chlorate, nitric acid and potassium permanganate which produce toxic gases (Lotya et al. 2009). Conversely, bottom-up approaches use molecules or atoms as building blocks of a complex structure and are considered very promising since these involve no wastage of materials (Biswas et al. 2012). The processes include epitaxial growth (Lee et al. 2019), chemical vapor deposition (CVD) (Wang et al. 2020), plasma-enhanced chemical vapor deposition (PECVD) (Jacob et al. 2015; Alancherry et al. 2020) and atmospheric pressure microwave plasma synthesis (Toman et al. 2021).

In vapor deposition techniques, a precursor in the form of gases is sent into a reaction chamber set at a higher temperature. When gases are exposed to the substrate, a reaction occurs and a monolayer to a few layers of graphene are created on the surface of the substrate. CVD, also known as thermal CVD, involves a high temperature of about 1000 °C (Muñoz and Gómez-Aleixandre 2013). However, with the assistance of plasma, graphene can be grown at lower temperatures ranging from 600 to 800 °C. The plasma generates an enormous chemical environment, producing a mixture of molecules, radicals and ions from hydrocarbon precursors, as a result facilitates lower formation temperatures and a faster synthesis process than thermal CVD (Boyd et al. 2015). The atmospheric pressure plasma is the state-of-art technique in which synthesis is carried out at atmospheric pressure; rendering it a substrate-free process without the need for high vacuum or temperature. This literature review focuses on PECVD and atmospheric pressure microwave plasma synthesis of graphene. Particularly, the parameters involved in the synthesis of graphene and their role in the structure of the graphene are addressed. Lastly, a detailed outlook on these techniques is provided as well.

2 Carbon nanostructures

The carbon allotropes of the nano-sizes comprising different shapes, sizes and dimensionality are widely sought-after research materials. This is due to their diverse properties, structural diversity and myriad of applications (Peng et al. 2012; Hahm et al. 2012; Novoselov et al. 2012; Liu et al. 2017). Until now variety of carbon nanostructures have been developed, and many efforts have been made to tailor the properties of those materials for targeted applications (Hatakeyama 2017). These nanoscale carbon structures can be classified based on their dimensionality i.e., zero, one and two-dimensional carbon nanostructures. Their division is shown in Fig. 2.

2.1 Zero-dimensional carbon nanostructures

Zero-dimensional carbon nanostructures include fullerenes, carbon dots or graphene quantum dots. The first synthesis of fullerenes was reported in 1990, where it was prepared by evaporation and recondensation of graphite (Krätschmer et al. 1990). Now fullerenes is prepared massively and thus easily available. Fullerenes have many interesting characteristics. For instance, the delocalization of charges
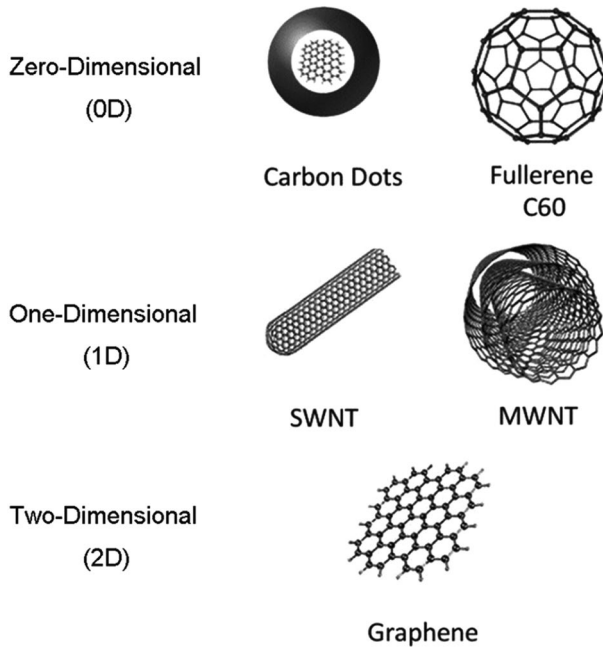
Fig. 2 Types of Carbon nanostructures (Liu et al. 2017)

within spherical carbon network and aromatic p-sphere are important for stabilizing charged units (Al-Jumaili et al. 2017).

Carbon dots or graphene quantum dots are the recent addition in zero-dimensional carbon nanostructures. The very first reported fabrications of these materials were from candle soot (Liu et al. 2007) and laser ablation method (Sun et al. 2006). However, now a variety of techniques have developed to synthesize carbon dots which include hydrothermal and electrochemical methods, and pyrolysis or microwave conversion of waste materials (Gao et al. 2014). The luminescence of carbon dots spans into the visible spectrum (Baker and Baker 2010).

2.2 One-dimensional carbon nanostructures

Carbon nanotube is a one-dimensional allotrope of carbon. Carbon nanotube is basically a cylindrically tube which can be obtained by rolling the graphene film (Zhang and Li 2009; Iijima 1991; Avouris et al. 2007). Carbon nanotubes are two types, single-wall carbon nanotube (SWCNT) (Niyogi et al. 2002) and multiwall carbon nanotube (MWCNT) (Lehman et al. 2011). Carbon nanotube offers interesting properties such as semiconductor, semi-metallic and metallic which make them an ideal material for sensing applications (Yang et al. 2010; Allen et al. 2007; Kauffman and Star 2008). The synthesis of carbon nanotube is usually obtained through chemical

vapor deposition method due to great merits of this method (Li et al. 2022; Wu et al. 2020).

2.3 Two-dimensional carbon nanostructures

The newest example of two-dimensional carbon nanostructure is graphene (Geim and Graphene 2009). Graphene is basically an atomically thin single layer of carbon hexagonal structure (Huang et al. 2017a). Graphene has myriad of applications due to its extraordinary properties, such as highest electron mobility, high surface area, and excellent conductivity, stronger than diamond etc. (Al-Jumaili, et al. 2022). Owing to this, extensive research has been devoted on developing the preparation methods of graphene. CVD (Muñoz and Gómez-Aleixandre 2013; Deng et al. 2019a), PECVD (Yang et al. 2013), epitaxial growth (Hass et al. 2008), Hummers method (Yu et al. 2016) and mechanical exfoliation (Martinez et al. 2011) are widely used methods to produce this two-dimensional material.

In addition to pristine graphene, various surface-treated forms of graphene i.e. graphene oxide, reduced-graphene oxide, photoluminescent graphene oxide, nitrogen-doped graphene/graphene oxide have also been developed (Liu et al. 2017). Graphene oxide is rich with oxygen functional groups such as hydroxyl, carboxyl, and epoxy groups (Chen et al. 2020a). Due to these oxygen functional groups, a negative charge is developed on the surface of the graphene. The non-altered areas of graphene contains free p-electrons, allowing p-interactions. The charge, surface chemistry, and hydrophilicity of graphene oxide add interesting properties in the graphene (Dreyer et al. 2010; Mao et al. 2013).

3 PECVD synthesis of graphene

The PECVD process for the synthesis of graphene can be divided into three parts, i.e., precursor delivery, decomposition, and graphene formation. A precursor in the form of gas is supplied into the plasma region, where it breaks down into smaller reactive reagents i.e., C, H, H_2, or CO, etc. depending on the composition of the precursor. Carbon in the form of graphene is deposited on the substrate, whereas, the residual gases flow out from the plasma region. The entire process is completed within a few seconds (Hatakeyama 2017; Dato 2019). Upon cooling, graphene deposited substrates are collected from the chamber and are well-kept for further investigations.

The PECVD reaction process is fast and efficient; however, it involves several factors influencing the process. For example, process parameters such as plasma power, precursor flow rate, chamber pressure, substrate temperature, etc. affect the synthesis method significantly (Al-Jumaili et al. 2022; Li et al. 2016a). An overview of the method is shown in Fig. 3. The next section will address these factors, explaining how they have been used in the past and their impact on the quality of graphene.
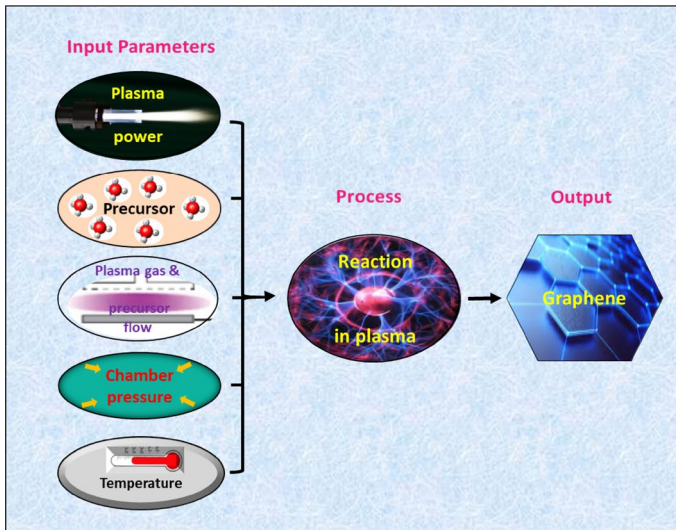
Fig. 3 An overview of the PECVD process to synthesize graphene

3.1 Input parameters

3.1.1 Plasma power

Plasma sources such as radio frequency (RF) and microwave (MW) in the frequency range of 1–500 MHz and 0.5–10 GHz respectively, and direct current (dc) plasma are commercially available to be utilized in different applications. For the synthesis of graphene, most researchers prefer using RF and MW at the frequencies of 13.56 MHz and 2.45 GHz respectively (Li et al. 2016a). These are standard industrial frequencies and are considered optimum values for the quality of the product (Vollath 2008). Both types of plasmas have been optimized for different powers and have shown quality results.

Nang and Kim (Nang and Kim 2012) studied the effect of RF power on the synthesis of graphene on Cu substrate from CH_4 precursor. For this purpose, the substrate was first preheated at 950 °C. Then among 50, 200, 400, and 600 W they reported 200 W, as a suitable power for quality production of graphene. Unlike RF plasma, high power of the microwave, typically above 1 kW was used to synthesize the graphene (Hiramatsu et al. 2013; Kalita et al. 2012; Kim et al. 2011a; Kumar et al. 2013; Malesevic et al. 2008). However, it should be noted that contrary to RF plasma, no substrate pre-heating is involved in microwave plasma. In the substrate-free synthesis of graphene using microwave plasma, (Dato et al. 2008) varied the plasma power from 350 to 1100 W and determined that the change in power had no substantial effect on graphene synthesis. It was noted that the low power of plasma was sufficient to produce the required quality of graphene.

3.1.2 Precursor

Precursor, also known as monomer or feedstock plays a vital role in the synthesis and properties of graphene. It has been found that the properties of synthesized graphene are not only affected by the composition of the precursor but also the flow rate of the precursor (Dato 2019). Therefore, scientists have investigated varieties of precursors. The key point in all precursors is that they must contain carbon compounds (Kumar et al. 2016). The fragmentation of a precursor is the primary step in all PECVD processes. The fragmentation process of a hydrocarbon precursor is highly endothermic and thus require a high temperature. Because of this process, the carbon will form graphene on the substrate. The by-products in the reaction are H_2 and CO, depending on the composition of the precursor. Some have used carbon-based chemicals, which are fossil fuels. These include but are not limited to methane (CH_4) (Guermoune et al. 2011; Wassei et al. 2012; Zafar and Jacob 2022), toluene (C_7H_8) (Zhang et al. 2012), xylene (C_8H_{10}) (Kumar et al. 2014), hexane(C_6H_{14}) (Gao et al. 2012), ethylene (C_2H_4) (Somekh et al. 2014), ethanol (CH_3OH), methanol (C_2H_5OH) (Guermoune et al. 2011), acetylene(C_2H_2) (Qi et al. 2013) etc. The hydrocarbons are usually mixed with hydrogen before they are supplied into the chamber. These precursors, mostly produced by fossil decomposition are highly toxic as well as prone to depletion over time.

Lately, renewable hydrocarbon-based precursors have been used which are found in enormous amounts on earth. The prime benefits of using these precursors are that they are easily accessible and can keep the reaction process green. To date, following precursors have been used; sesame oil (Kumar et al. 2014), *Melaleuca alternifolia* is commonly known as tea tree (Jacob et al. 2015), camphor (Sharma et al. 2013), turpentine (Awasthi et al. 2010), geranium (Al-Jumaili, et al. 2022), eucalyptus (Li et al. 2017), palm (Nasir et al. 2017), and soybean oil (Seo et al. 2017). Moreover, eatable products such as honey, biscuits, sugar, milk, and cheese have excitedly shown the viability of being potential precursors for the synthesis of graphene (Seo et al. 2013a).

Overall, it has been found that the used precursors can be in solid, liquid, and gaseous forms. Nonetheless, the results have shown that the quality of graphene is far better in gaseous precursors compared with solids or liquids (Deng et al. 2019a).

3.1.3 Gas and precursor flow

Hydrogen (H_2) gas in combination with a precursor is generally used in the synthesis of graphene. Only a few have used argon (Ar) without H_2, however, the quality of graphene is compromised in this method (Peng et al. 2013; Wang et al. 2011). The proportion of gas relative to that of the precursor also has a significant effect on the synthesis process. Not only does it determine the final product, i.e., carbon nanotube (CNT), graphite, and/or graphene but also plays a role in shaping the morphology and structure of the graphene (Bo et al. 2013). (Wu et al. 2004) studied the effect of the H_2/CH_4 ratio in synthesis on gold (Au) substrate. Using the MW-PECVD at temperatures between 650 and 700 °C, and varying only H_2 concentration, they found considerable impact of H_2 gas on synthesis. A higher concentration of H_2 i.e., H_2

/CH_4 ratio of 100, which is used for diamond film formation, showed no observable outcome. Decreasing the ratio to 30 showed some columnar structures, further decrease showed a mixture of fibers/tubes and graphite nanosheets. Additional lowering of the ratio to reach the range of 4–8 produced vertical graphene nanosheets. (Wang et al. 2004) studied the effects of CH_4 concentration by varying it from 10 to 100% in H_2 atmosphere. They used an RF plasma system at the power of 900 W while changing substrate temperatures from 600 to 900 °C. All specimens yielded the same vertically standing graphene flakes of similar thicknesses. However, with the increase of CH_4 concentration, the size of sheet decreased; meanwhile the density of graphene decreased as well. Generally, gas ratio of CH_4/H_2 higher than 1:20 is depicted as optimum for vertical graphene synthesis in PECVD (Bo et al. 2013).

Hydrogen, either mixed with inert gasses (argon or helium) or in pristine form, play a vital role in the synthesis of graphene film on a substrate. Hydrogen acts as a catalyst and controls the grain size and shape by etching away the weak carbon bonds. Hydrogen partial pressure also affects the number of layers of graphene. It also has been noted that in the absence of hydrogen, graphene might not form (Vlassiouk et al. 2011).

3.1.4 Chamber pressure

The chamber pressure has shown remarkable influences on the production rate of graphene. For instance, sub-atmospheric pressure has a low production rate while high vacuum pressure is favorable to attain a high production rate in microwave plasma. It happens, because the collisions between electrons and heavy particles which causes high temperature, is a key part of the process. Sub-atmospheric plasma does not favor this collisional phenomenon, hence a rise in temperature does not occur which eventually slows down the graphene synthesis (Dato 2019). However, to get high-quality graphene, without any impurities, it is important to vacuum the chamber. In literature, a wide range of chamber pressures has been used. It includes high vacuum pressure, low pressure (0.01–0.02 mbar), and atmospheric pressure (1014 mbar) (Muñoz and Gómez-Aleixandre 2013).

3.1.5 Temperature

Temperature is an essential factor in any graphene synthesis process. Depending on C-H bonding energy, temperature also varies from one precursor to another. Compared with thermal and CVD processes, the PECVD process can be performed at lower temperatures. It is due to the presence of active ions and energetic electrons which can assist in breaking down the chains of molecules (Dato 2019). Based on the plasma source, some PECVD processes require precursor and/or substrate heating. In dc glow discharge, the substrate as well as the precursor must be heated. MW and RF-PECVD also require substrate heating. However, some of the MW plasma systems do not rely on the heating of the precursor or the substrate (Bo et al. 2013).

The substrate is heated externally, thus an additional heating element is coupled with the quartz tube. The heating temperature of the substrate depends on the conditions of other parameters. In most of the studies, substrate temperature usually

differs from 600 and 1000 °C. (Rao et al. 2009) have shown a very low substrate temperature i.e., 400 °C for the synthesis of carbon nanostructures. In another study, it was revealed that graphene could not be produced at a temperature below 600 °C. In addition, the substrate temperature happens to have an effect on the density of the synthesized graphene. Higher temperatures, for example, more than 730 °C produced high-density graphene (Bo et al. 2013). Apart from substrate temperature, plasma generation also causes some increase in the temperature. Therefore, at the time of reaction, the temperature inside the chamber is always higher than the measured substrate temperature (Rincón et al. 2015).

3.2 Process

RF and MW plasma are widely studied plasma sources. The main role of plasma is twofold, i.e., heat transfer and transfer of momentum to breakdown the chains of precursor molecules. This role helps to lower the pre-heating temperature of the substrate. Here, the past work on RF and MW-PECVD, categorizing them based on different substrate temperatures, will be analyzed.

3.2.1 Radiofrequency PECVD

3.2.1.1 Low temperature (< 600 °C) (SEO et al. 2013b) produced graphene without any substrate by heating butter on Ni foam; where butter was used as a precursor. They used a high 1000 W plasma power, which can build a temperature from 400 to 450 °C. The Raman spectroscopy results showed evidence of some graphene. However, the quality of graphene was compromised, as the D peak, which indicates the number of defects, was quite high. (Chen et al. 2015a) attempted to synthesize graphene at a quite low temperature of 300 °C and studied the effects of deposition time on the thickness of graphene. Their results presented graphene of thickness varying from 10 to 600 nm, which is higher than most reported thicknesses of graphene. The Raman spectra also did not produce the desired outcome as the D peak was quite higher and the 2D peak was quite lower than the G peak. Moreover, the lengthy synthesis time of 60 min also renders this approach unsuitable for graphene synthesis.

3.2.1.2 Medium temperature (600–750 °C) (QI et al. 2011) produced 1–3 layers of graphene on a Si/SiO_2 with Ni film-substrate at low temperatures. It can be attributed to the fact that the plasma power leads to the formation of a high concentration of radicals on the surface of Ni, which in turn promotes carbon growth on the surface. Likewise, (Wang et al. 2010) adopted the same parametric approach using relatively medium temperatures. They used Cobalt (Co) as a substrate. In their results, they mentioned that Co has a vital role in synthesizing better quality graphene.

(Vizireanu et al. 2008) performed a parametric study and found that the gas mixture $Ar/H_2/C_2H_2$ flow rate has a noteworthy influence on the morphology of graphene. In addition, temperatures greater than 600 °C, plasma power between 250 and 400 W, and the argon mass flow rate greater than 500 sccm are important factors for graphene growth. Song et al. (Song et al. 2014) produced graphene on different

substrates i.e., Si, SiO$_2$, Quartz, gallium arsenide (GaAs), germanium (Ge), and carbon fiber (C_f). They successfully accomplished a homogeneous vertical graphene distribution on all substrates. Good quality graphene at medium temperatures is reported by Zhu et al. (Zhu et al. 2007), who used RF plasma at 680 °C and deposited nanosheets directly on a Ni wire.

3.2.1.3 High temperature (> 750 °C) (KATO et al. 2016) performed high-temperature PECVD process and analyzed the effect of temperature on graphene nucleation and growth rate. High-density graphene grains were observed at 750 °C, which start growing with the increase in temperature. At a temperature of 950 °C, they found a single graphene grain. However, unlike the ones observed at 800 and 850 °C, the graphene grain at 950 °C was not hexagonal.

Terasawa and Saiki (Terasawa and Saiki 2012) found that the substrate temperature has a great impact on graphene layers. The substrate temperature of 500 °C produced multilayer graphene, whereas they detected a monolayer at 900 °C. Moreover, crystallinity is higher at temperatures greater than 900 °C. (Ma et al. 2019a) studied the effect of gas pressure on graphene synthesis at a higher temperature. For instance, the growth rate of graphene at 950 °C temperature and 1.2 torr pressure is slower than that at 570 mTorr. It is mainly due to the slower carbon supply from the gas phase to the substrate.

(Ma et al. 2019b) studied the effects of plasma power source and growth temperatures on the morphology of vertically grown graphene. Varying the power source from 80 to 280 W, they noticed vertical graphene flakes forming a bush-like shape. They named it a tree-like structure as it appeared like one when seen from above in SEM microscope. Similarly, varying the temperature of the substrate from 700 to 850 °C greatly influenced the tree-like morphology. When the temperatures are lowered, the distance between each tree is reduced prominently, while the height of tree-like structure increases. The flakes of graphene in tree-like structure become interlinked. Resultantly, porous films of graphene are obtained at lower temperatures.

Among low, medium, and high temperature, it is believed that irrespective of precursor type, medium temperature range, i.e., 600–750 °C is appropriate for graphene synthesis. Low temperatures require either high plasma power or demand a long processing time. Higher temperature ranges do not make the process suitable for the substrates, which have low melting temperatures. Thus, a medium temperature range assisted with medium plasma power is adequately suitable for graphene synthesis.

3.2.2 Microwave PECVD

(MALESEVIC et al. 2008) produced highly crystalline graphene on various substrates such as quartz, silicon, nickel, steel, titanium, etc. Overall, similar results were observed on all substrates. However, different flakes adhesion was indicated which could be attributed to the carbide formation on the substrate. (Yamada et al. 2013) also used the MW-PECVD process to synthesize graphene at a low temperature such as 320 °C accompanied by no substrate heating. They displayed successful graphene synthesis for optoelectronic applications due to the high optical

transmittance and sheet resistance. The production of graphene at this lowest temperature on a non-catalytic aluminum substrate was an extraordinary achievement.

(Yuan et al. 2009) also synthesized graphene using MW-PECVD; however, they used higher temperature by heating the substrate with an inductive heater. In their results, they found crystalline graphene with some defective morphology. (Vitchev et al. 2010) studied the growth of graphene on different substrates, produced using MW-PECVD. On the initial synthesis stage, they found SiC formation on a silicon substrate, which was not seen on quartz, or platinum (Pt) substrates. At later stages of growth, they observed a similar formation phenomenon in which layers of graphene flakes were developed. (Kalita et al. 2012) prepared graphene film at the lowest temperature of 240 °C. The results, however, showed some defects, which render this lower temperature unsuitable for synthesis.

(Kim et al. 2011a) studied the synthesis of graphene at various temperatures. Consequently, they found monolayer graphene in the temperature range of 450 °C to 750 °C. The outcome was the creation of centimeter-scale graphene with the characteristics of high transparency and low sheet resistance i.e., 590 Ω/sq. However, graphene formed below 450 °C had numerous defects, making it undesirable for applications.

MW-PECVD has also been used to dope the graphene sheets. For instance, (Kumar et al. 2013) produced an N-doped graphene film up to the concentration of 2 atomic percent. For this purpose, an additional supply of nitrogen gas was provided in a microwave plasma system. Nitrogen gas was released for a minute when precursor (CH_4) was released. This fast and efficient process of N-doping showed the potential to produce p-doped graphene as well.

3.3 Growth mechanism of graphene

The growth of vertical graphene using RF-PECVD process has been studied by (Wang et al. 2014). In their findings, they delineated a three-step formation process, i.e., (i) nucleation and island formation of carbon film, (ii) initial growth of graphene sheets, and (iii) further growth and net-like formation of graphene sheets. A schematic representation of graphene growth processes and SEM images taken during the growth process are shown in Fig. 4.

Similarly, (Malesevic et al. 2008) also identified the three-step graphene growth process as shown in Fig. 4.1 and 4.2. Firstly, a graphite layer is made parallel to the substrate surface and seen as a crack on the surface. In the second stage, freestanding graphene nucleation starts from these cracks in the vertical direction. The growth of these vertical graphene continues due to the accumulation of carbon radicals on the edges of these graphene.

A recent study by (Zhang et al. 2016) also mentioned the similar three stages of graphene growth on Si substrate. However, they observed the growth of the buffer layer (SiC) parallel to the substrate's surface before the nucleation of vertical graphene flakes from the defects. However, the defect formation such as cracks on the surface of the substrate is beneficial for graphene growth as it provides highly active sites for nucleation.
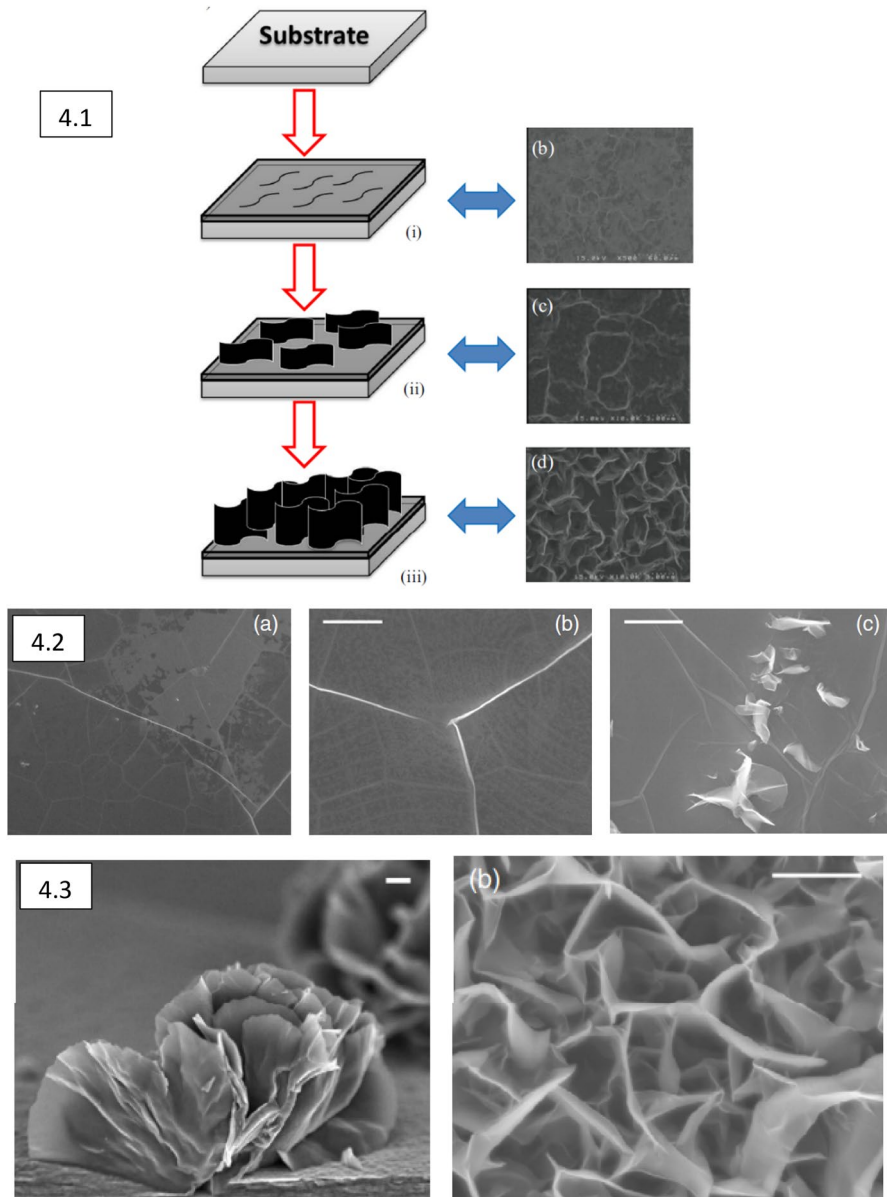
Fig. 4 (4.1) Three stages of graphene nucleation and growth (Wang et al. 2014), (4.2) Three-step growth mechanism of graphene (Malesevic et al. 2008), (4.3) High-resolution SEM images of graphene (Malesevic et al. 2008)

Nevertheless, it should be noted that the final quality of graphene highly depends on the process conditions such as type of plasma source, process parameters, growth and cooling time, etc. The process conditions bring about differences in graphene

Table 1 Atmospheric pressure microwave plasma synthesis of graphene

Power	Precursor Type	Flow rate	Feeding mechanism	Plasma gas and flow rate	Production rate (mg min^{-1})	References
250 W	Ethanol	4×10^{-4} L/min	Aerosol	Ar, 1.71 L/min	2	(Dato et al. 2008; Dato et al. 2009)
250–1050 W	Ethanol, methanol, isopropyl alcohol (IPA), dimethyl ether (DME)	4×10^{-4} L/min	Aerosol	Ar, 6.8 L/min	–	(Dato and Frenklach 2010)
250–1050 W	Ethanol	4×10^{-4} L/min	Aerosol	Ar, 3.4 & 1.71 L/min	6	(Dato and Frenklach 2010)
400–900 W	Ethanol	0.5–3.5 sccm	Aerosol	Ar, 250 to 2000 sccm	2	(Tatarova et al. 2013)
500–900 W	Ethanol	0.6–3.5 sccm	Aerosol	Ar 250 sccm	–	(Tatarova et al. 2014)
400–1000 W	Ethanol, methane	0.6–10 sccm	Aerosol	Ar, 250–1500 sccm	–	(Tatarova et al. 2016)
500–2000 W	Ethanol	5–30 sccm	Aerosol	Ar, 1000–1500 sccm	2	(Tatarova et al. 2017)
200 W	Ethanol	0.22 g/h	Aerosol	Ar, 0.75 L/min	0.07	(Rincón et al. 2015)
300 W	Ethanol	2 g/hour	Aerosol	Ar, 1 L/min	1.33	(Melero et al. 2017)
–	Ethanol	1 mL/min	Direct spray	Ar, 5 slm	–	(Bertin et al. 2019)
1 kW	Methane	2–8 sccm	–	Ar, 600–2000 sccm	–	(Bundaleska et al. 2018a)
700–900 W	Ethanol	0.6 sccm	Aerosol	Ar, 250 sccm	–	(Tsyganov et al. 2015)
–	Ethanol	0.1–1.5 mL/min	Direct spray	Ar (5–14 slm)+H2 (1–1.5 slm)	–	(Münzer et al. 2018)
1.2–1.4 kW	Methane	–	–	Ar	–	(Singh et al. 2019a)
250 W	Ethanol	2×10^{-4} L/min	Aerosol	Ar, 1.71 L/min	–	(Nakahara et al. 2020)
300 W	Ethanol	48.3 mg/min	Aerosol	Ar, 1 L/min	1.45	(Casanova et al. 2021)

morphology, density, and microstructure. As evident from the different names given to the final morphology of graphene, it can be referred to as petal, bush or tree-like, turnstile, cauliflower, and maze-like structure (Chen et al. 2015b).

4 Atmospheric pressure microwave plasma synthesis of graphene

Atmospheric pressure plasma synthesis is a substrate-free synthesis in which free-standing graphene is produced on a gram scale within a few seconds. The formed graphene is collected downstream on membrane filters or from the walls of the reaction chamber (Lee et al. 2019; Dato 2019; Tatarova et al. 2013). In the following discussion, salient features of this process (summarised in Table 1) will be discussed.
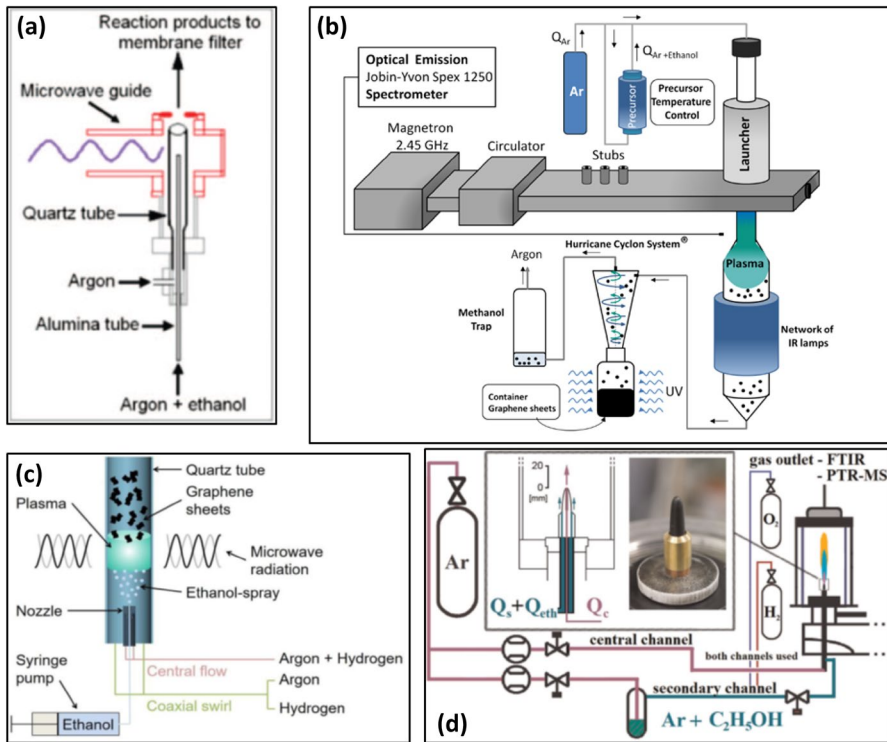
4.1 Plasma reactors

Atmospheric pressure microwave plasma has been previously used to synthesize boron nitride or aluminum nanoparticles. For graphene, (Dato 2019) were the first to show the possibility of synthesis of free-standing graphene in a similar reactor. They used a quartz chamber, which has an alumina tube concentrated in a quartz tube. The alumina tube was used to deliver carbon precursor i.e., ethanol, directly into the plasma stream. The schematic illustration of their system is shown in Fig. 5a. The dissociation of ethanol vapors and their conversion into solid matter occurred in a short interval, and a 2 mg/min production rate was recorded.

(Tatarova et al. 2013) used surface wave-induced microwave plasma to synthesize free-standing graphene. Considering the crucial role of outlet plasma stream, they modified the system with a cryostat to control the temperature at the nucleation zone. With small modifications, they used the same system for the synthesis of N-doped graphene as well. Briefly, it consists of a 2.45 GHz generator, which is connected with the waveguide, quartz tubes, and hurricane cyclone system followed by a methanol trap. They actively controlled the gas flow rate and temperature by MKS247 Readout and infrared irradiation of the wall respectively. Vaporization was performed by passing argon gas through an ethanol tank (Tatarova et al. 2017). The system is shown in Fig. 5b.

(Melero et al. 2017) used a special microwave plasma torch, named as TIAGO (Torche a Injection Axiale sur Guide d'Ondes, in French) torch. It is a one-nozzle component, providing a single flame of plasma. The torch supplied with argon gas opens inside a quartz chamber and forms plasma having the appearance of a jet conical flame. They adjusted the system with efficient argon and precursor input i.e. ethanol mixer system, which allowed the control of ethanol vapors supply. The Controlled Evaporator Mixer (CEM, Bronkhorst) along with the ethanol vaporization system is superior to bubblers in terms of stability and accuracy.

(Münzer et al. 2018) used the same approach as (Dato 2019) and (Tatarova et al. 2013) as shown in Fig. 5c. However, they supplied ethanol using an external syringe pump at an optimized flow rate. Moreover, they also investigated the effect of reactor's pressure by varying it from 1000 to 1500 mbar.

Fig. 5 **a** Schematic illustrations of plasma reactors used by (Dato et al. 2008) **b** (Tatarova et al. 2017) **c** (Münzer et al. 2018) **d** (Toman, et al. 2021)

(Toman, et al. 2021) synthesized graphene in a dual-channel microwave plasma torch at atmospheric conditions. The setup is shown in Fig. 5d. The system was fixed with two supply channels i.e. central and secondary channels for argon and argon-ethanol mixture respectively. The advantage of this specific design is that the system can also be fed with oxygen and/or hydrogen gasses through the central or secondary channel. The precursor flow was controlled by the mass-loss method, which may not have had a precise and active control on ethanol vapors. Nonetheless, an efficient method for the collection of graphene nanosheets is needed, as the collection from the walls of the container is tiresome for upscaling of the method.

4.2 Precursors and their role in graphene formation

Few precursors have been explored for microwave plasma synthesis of free-standing graphene. (Dato et al. 2008; Dato and Frenklach 2010) employed different precursors and investigated their role in shaping the final morphology of graphene. They supplied precursors into the plasma in an aerosol form. Their main study was on investigating ethanol as a precursor, however, they also studied methanol, isopropyl alcohol (IPA), dimethyl ether (DME). The methanol feed

showed no apparent formation of substances. It could be due to two possibilities; either plasma power was not enough to breakdown the methanol into its constituents or only gas substances were formed which escaped the outlet of the reaction chamber. On the other hand, IPA formed carbon soot, whereas, DME showed encouraging results for graphene synthesis.

Ethanol is the most commonly used precursor in the gas-phase synthesis of graphene. In (Dato et al. 2008) work, ethanol formed single and bilayers graphene nanosheets at a microwave power of 250 W at the rate of 2 mg/min. (Tatarova et al. 2013) made graphene having 1–5 number of layers from ethanol at a microwave power of 900 W. Similarly, (Melero et al. 2017) observed 2–7 layers of graphene from ethanol at a microwave power of 300 W. In their work, ethanol produced 1.33 mg/min of graphene from 33 mg/min of ethanol consumption, which is comparable with the findings of (Dato et al. 2008), where they obtained 2 mg/min graphene but at the cost of 3 times higher ethanol consumption.

The composition of the precursor especially C/O ratio has a profound effect on graphene formation (Dato and Frenklach 2010). It was noted that to develop C–C bonding in graphene, a suitable amount of carbon is necessary. Since the C/O ratio in methanol (CH_3OH) is one, it is more likely to produce CO instead of C–C bonding. On the other hand, a higher C/O ratio as in the case of IPA (C_3H_8O) will form carbon soot. The C/O ratio in ethanol (C_2H_5OH) has been reported to be appropriate to initiate C–C bonding. DME (C_2H_6O), which has the same C/O ratio as ethanol, showed promising results for graphene synthesis. A single carbon is deemed insufficient to give forth C–C bonding, instead it may form CO. The above description also highlights the significance of the presence of oxygen in the formation of graphene as well as overall production rate.

Encouraging results on graphene formation have been reported using methane (CH_4) as the only source of carbon at a microwave power of ~1 kW (Bundaleska et al. 2018a; Singh et al. 2019a). Interestingly, methane, which carries only one unit of carbon negates the fact that carbon should be in C–C form to produce graphene. However, it should also be noted that the O in methane is absent and CO formation might not happen.

The influence of the flow rate of ethanol and plasma gas on the structure of synthesized products has also been analyzed. (Tatarova et al. 2013; Tatarova et al. 2014; Tatarova et al. 2016) studied the effect of aerosol flow rate ranging from 0.5 to 3.5 sccm. A flow rate of 0.6 sccm for ethanol and 250 sccm for Ar showed the highest quality graphene. In another study, (Tatarova et al. 2017) raised the ethanol flow rate to 30 sccm, and Ar to 1200 sccm to synthesize graphene. It was suggested by them that a short precursor residence time would avoid the agglomeration of graphene into graphite. They observed ethanol decomposing into C, H, H_2, C_2, and CO (Tatarova et al. 2014). (Dato et al. 2008; Dato and Frenklach 2010) mentioned the formation of CO, C_2, and H_2 as well. However, they linked C_2 formation with the C/O ratio of the precursor. In mass spectrometeric analysis, (Rincón et al. 2015) observed CO, H_2, and traces of acetylene and methane as a by-product. (Münzer et al. 2018) synthesized high quality and largest quantity of graphene at 1 mL/min flow rate of ethanol. (Singh et al. 2019a) added hydrogen

in the precursor to study the influence of hydrogen on graphene structure. They found that higher the ratio of H/C, greater would be the yield of graphene.

The role of oxygen in the synthesis of free-standing graphene using microwave plasma has also been investigated. It was found that the reactant concentration has a great influence on the graphene formation. The low content of the reactant concentration reduces the soot formation, and promotes the graphene production. The amount of water in the precursor promotes CO formations, and hence the graphene formation (Fortugno et al. 2022).

4.3 Microwave power

Microwave power plays an important part in dissociating the precursor and raising the electron temperature in the plasma chamber (Dato and Frenklach 2010). A range of microwave powers, for instance, as low as 250 W (Dato et al. 2008) and as high as 2 kW (Tatarova et al. 2017) have been investigated to synthesize graphene. It has been noted that for ethanol precursors, the microwave power does not significantly affect the structure of graphene. Graphene was formed at all microwave powers. However, other alcoholic compounds, such as isopropyl alcohol, start forming soot-like carbonaceous particles at higher microwave power (Dato and Frenklach 2010).

In another study on the synthesis of graphene from ethanol, (Tatarova et al. 2014) observed that decreasing the power below 500 W formed carbon nanoparticles instead of graphene (Fig 6). They ascribed this to supersaturation occurring inside the chamber due to the decrease in gas temperature. However, the TIAGO torch operating at a low microwave power of 300 W revealed the formation of pure graphene consisting of a few layers (Melero et al. 2017). Thus, it can be stated that the design of the plasma reactors also carries a strong influence on the final structure of the carbon material.
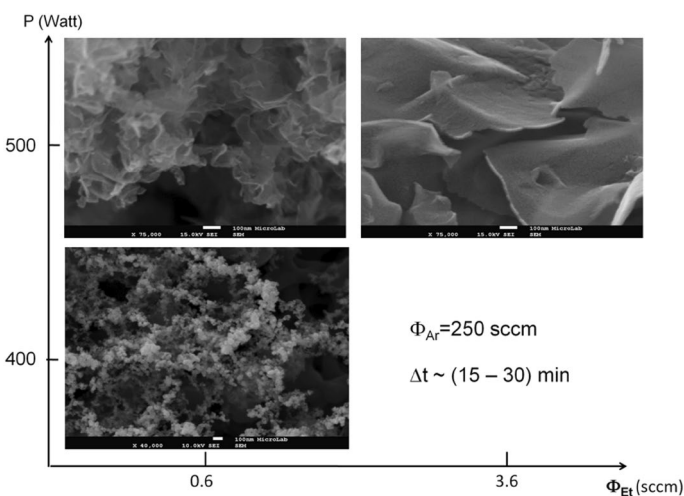

Fig. 6 Effect of ethanol flux and microwave power on carbon nanostructure (Tatarova et al. 2014)

(Bundaleska et al. 2018a) synthesized graphene from methane at a microwave power of 1 kW. Interestingly, the same microwave power of 1 kW but with higher methane and Ar flow rates formed diamond-like structures. They also developed a theoretical model, which indicated the formation of solid carbon compounds at higher microwave powers such as 1.5 kW. (Toman, et al. 2021) have studied the influence of the microwave power on the structure of graphene. They reported that the transition of material from amorphous to crystalline form depends on the microwave power, ethanol flow rate, and molecules mixture.

4.4 Comparison of the graphene structure and morphology

(TATAROVA et al. 2014) controlled the wall temperature of the plasma chamber using a cryostat and studied its influence on the quality of graphene. It was noted that external heating or cooling does have some effect on the structure of graphene. For instance, low wall temperatures form carbon nanoparticles, whereas temperatures above 60 °C promote graphene formation. Also, the samples showed lower number of monolayers when the wall temperatures were kept above 60 °C. However, the Raman spectra shown in Fig. 7 displayed an intense peak for the wall temperature of 60 °C as compared to that of 80 °C. This can be attributed to the structural defects in the samples created at 60 °C. The low-resolution images shown in Fig. 7 showed monolayers and a few layers of graphene nanosheets. In addition, it can be observed that some of the sheets are overlapping and folded at the edges.
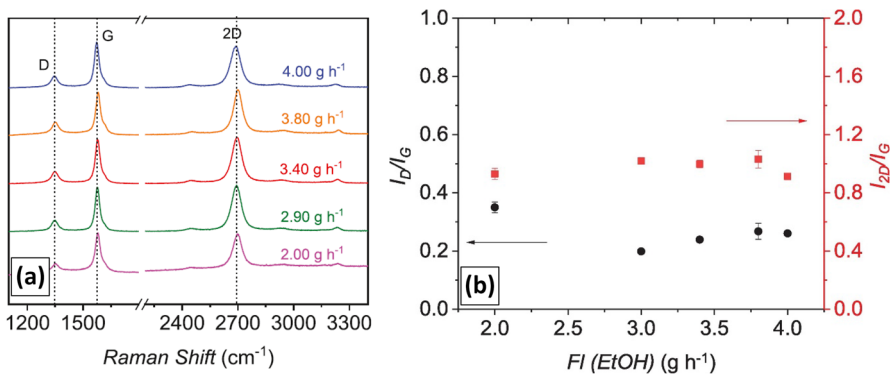
The effect of precursor flow rate on the quality and production amount of graphene has also been investigated thoroughly. In a work presented by (Casanova et al. 2021), they found that varying the ethanol flow rate from 2 to 3.4 g/hr, increases graphene production steadily. However, a further rise in ethanol flow rate not only reduces the quantity of graphene but also starts forming carbonaceous particles. This can be illustrated through the Raman spectra (shown in Fig. 8a, b) which also shows the intensity ratios i.e., I_{2D}/I_G and I_{2D}/I_G at different ethanol flow rates. Only 4 g/hr flow rate of ethanol showed I_{2D}/I_G value of less than one, which is indicative of multilayer graphene. However, a 3.4 g/hr flow rate of ethanol can be considered optimum parameter in this synthesis since the value of I_D/I_G, which suggest the defects in the structure, is the lowest. Overall, all the samples of different ethanol flow rates showed evidence of graphene formation. The D (~ 1350 cm^{-1}), G (~ 1580 cm^{-1}) and 2D (~ 2700 cm^{-1}) bands can be observed in Fig. 8. The low values of I_D/I_G, ranging between 0.2 and 0.35 indicated the low number of defects in the sample. The shoulder peak in G band arises due to intra valley transition (Sukumaran et al. 2018) and corresponds to weak disorder-induced feature (Toth et al. 2015).

4.5 Synthesis of nitrogen-doped graphene

The scope of atmospheric pressure microwave plasma has now been extended to the synthesis of nitrogen-doped graphene (N-graphene). It has been proven that it is possible to synthesize a good quality N-graphene in a single-step using an atmospheric pressure microwave plasma system. However, the high-resolution N1s spectra
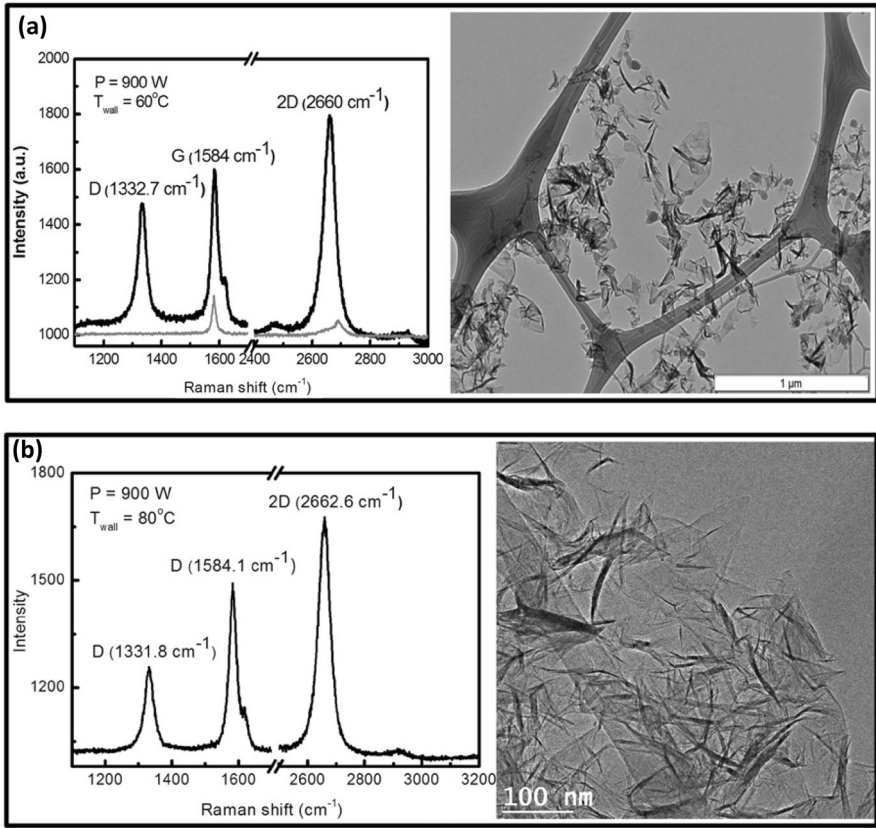
Fig. 7 Raman spectra and corresponding TEM images showing the effect of chamber wall temperatures (Tatarova et al. 2014)

Fig. 8 **a** Raman spectra of samples showing the effect of ethanol precursor flow rate, **b** I_D/I_G (black circles) and I_{2D}/I_G (red squares) values of the Raman spectrum obtained at different flow rate of ethanol (Casanova et al. 2021)

of these materials have revealed that the pyrollic N that is considered important for some applications was absent. Moreover, the procedure involved the usage of an additional nitrogen gas supply along with the consumption of a 2 kW high microwave power. This practice makes the process energy-intensive (Tatarova et al. 2017). In another attempt to synthesize in-situ N-graphene, (Bundaleska et al. 2018b) used ammonia instead of nitrogen along with ethanol. The high-resolution N1s results showed the presence of pyridinic, pyrrolic, and graphitic nitrogen. However, they also used a high microwave power of 2 kW. Moreover, ammonia being a toxic chemical is not an appropriate choice for the synthesis.

(Tsyganov et al. 2020) synthesized N-graphene by injecting ammonia directly into different zones of plasma. They found that the injection position plays a role in determining the doping level of nitrogen in graphene and the yield of N-graphene. Recently, another approach for single-step synthesis of nitrogen-doped graphene oxide (N-GO) has been reported (Zafar, et al. 2022). They eliminated the usage of any additional gas or precursor and synthesized the N-GO from aniline as a sole precursor. Also, they brought down the microwave power to 80 W, which was a substantial reduction in the usage of the energy. Moreover, their results exhibited the presence of nitrogen in the form of pyridinic, pyrrolic, and graphitic nitrogen. However, applications N-GO needs to be converted into N-graphene using additional steps such as reduction.

5 Other plasma sources for the synthesis of graphene

Various other plasma techniques depending upon the sources of plasma have also been employed to synthesize graphene. It includes DC plasma (Tu et al. 2013; Tzeng et al. 2013), cathodic vacuum arc plasma (Shen et al. 2012), thermal jet plasma (Kim et al. 2010; Lee et al. 2016), and hot filament/hot wire plasma (Singh et al. 2019b; Wang et al. 2015). Although the product of theses plasma sources i.e., graphene have nearly same characteristics, but the setup to produce graphene involves different parts and procedures. For instance, DC plasma setup consisted of graphite rod anode to hold the substrate, tungsten cathode, DC power supply, and quartz chamber (Yu et al. 2011). DC plasma system are also two types, i.e., pin to plate and parallel plate type. In DC plasma, it has also been reported that the distance between plasma source and substrate significantly affects the final structure of the graphene (Ghosh et al. 2017; Sahoo et al. 2022).

In hot-filament process two Tantalum filaments (0.5 mm diameter) fitted above the substrate, heated to 2000 °C are used to dissociate the gasses and to convert it into the graphene. (Zhai et al. 2020) synthesized B-doped graphene directly on glass substrate using hot-filament CVD method. The synthesized graphene consisted of nanocrystalline graphene grains and was uniform on the large scale of glass substrate. Radiofrequency thermal plasma jet system consisted of plasma torch, generator, quartz reactor, and a precursor delivery system. (Fronczak et al. 2022; Fronczak et al. 2017) showed continuous synthesis of graphene from different carbon sources in RF-thermal plasma. The proposed system produced a comparable graphene nanostructure.

Microplasma, a recently emerging technique is also a promising technique for the synthesis of graphene. Microplasma, featuring micro-scale dimensions is a low-temperature plasma, which comprises non-equilibrium reactive environment and high-energy density (Chiang et al. 2020). Microplasma has been employed to synthesize graphene quantum dots in colloidal form. The synthesis was carried out at atmospheric conditions. The graphene quantum dots had the average diameter of 4.9 nm, and showed photoluminescence around 448 nm (Yang et al. 2019a).

An inductively coupled plasma was used to synthesize and coat graphene on the stainless steel. In this novel approach, it was demonstrated how graphene can be sprayed on the substrate by employing a two-translation axis robotized arm. This system also allows a precise control over the distance between substrate and plasma torch, and substrate's plasma exposure time (Aissou et al. 2022).

6 Plasma for the synthesis of graphene-based composites

(WEI et al. 2014) synthesized graphene oxide and silver nanoparticles nanocomposite in dielectric barrier discharge plasma at ambient conditions. A reduction method was used for this purpose, where plasma worked as a reductant on a graphene oxide substrate. Briefly, first a mixture of graphene oxide and Ag nanoparticles powders were mixed ultrasonically for 12 h. After drying the mixture, it was reduced using hydrogen plasma for 1 h. However, it was a long procedure for the synthesis of nanocomposite, overall it was a green and dry process since it did not require any surfactants and solutions. The nanocomposite formation was confirmed through XRD, XPS and EDS elemental analysis. The as-fabricated nanocomposite was quite effective against escherichia coli bacteria.

In another study, rGO/Mn_3O_4 composite was prepared in dielectric barrier discharge plasma. First, Mn and GO were produced through Hummers method. Subsequently, they were converted into rGO/Mn_3O_4 composite using air oxidation and dielectric barrier discharge plasma deoxygenation. XPS, XRD and TEM confirmed the formation of nanocomposite. The synergistic effect of both rGO and Mn_3O_4 showed remarkable results in supercapacitor application. For instance, 193 F/g specific capacitance was noted when the amount of Mn_3O_4 was 90% in the composite (Jiangying et al. 2013).

Microwave plasma was used to synthesize Pt/graphene composite from the mixture of Pt and ethanol. The experiment was employed at ambient conditions. Raman, XRD and TEM were used to characterize the composite. The TEM images showed Pt nanoparticles of 2.6 nm sizes uniformly dispersed on graphene having wrinkled-paper like sheets. The Pt/Graphene composite had high surface area, which made it promising material for catalysts applications (Jo et al. 2016).

TiC/graphene nanocomposite was produced by (Kim et al. 2018) in thermal plasma. The results showed that TiC were less than 50 nm sizes, and well dispersed. In another study, graphene nanocomposite with anatase TiO has also been produced using the plasma. The synthesis was carried out in three steps, i.e. thermal plasma, dielectric barrier discharge (DBD) and heat treatment. In thermal plasma, TiC-graphene composite was synthesized from isopropoxide. Afterwards, it was converted

to anatase TiO_2 in dielectric barrier discharge plasma, followed by heat treatment to remove amorphous carbon and contaminants. The TEM images revealed 50 nm or below sizes of TiO_2 nanoparticles. Moreover, the dispersion of the TiO_2 nanoparticles were quite uniform on the graphene nanosheets (Heo et al. 2019).

(Tanaka, et al. 2020) synthesized graphene-encapsulated silicon nanoparticles using pulse-modulated induction thermal plasma with a controlled feedstock. Graphene was synthesized from methane in the induction plasma. Micro-sized Si particles were sent intermittently into the plasma. The formation of graphene-encapsulated Si nanoparticles was confirmed through SEM, XRD and TEM. This approach of synthesizing the graphene composite is commendable especially for its high production rate.

Another unique approach i.e. solution plasma process was used to synthesize $GO\text{-}MnO_2$ composite for a supercapacitor application. The process involves the generation of plasma in the beaker containing the mixture of GO and MnO_2. The plasma was generated by bipolar-DC power supply at ambient conditions. The as-synthesized GO/MnO_2 composite was used for a supercapacitor application which showed specific capacitance of 218 F/g (Pimklang et al. 2022).

7 Plasma-based processing of graphene structure

To achieve desirable properties in synthesized graphene, the structure of graphene can be altered using radio frequency or microwave plasma. The structure alterations include doping, intentional creation of pores, defects and/or functionalization. Depending on the exposure time, reactive radicals and ions in the plasma are responsible for the development of point and line defects in the graphene layers and thinning the reactive edges of the graphene (Ostrikov et al. 2013; Jagodar et al. 2022). The defects such as grain boundary and topological defects give rise to high strength in tilted graphene boundaries (Wei et al. 2012) and improved electronic properties (Botello-Méndez et al. 2011) respectively.

Plasma can be used for in-situ functionalization of graphene by introducing different gases in the reaction chamber. Hydrogenated graphene gives improved p-type conduction and physical properties. Also, it converts the semi-metallic graphene to insulator (Elias et al. 2009), and impart magnetic properties (Zhou et al. 2009). Increasing the doping amount of hydrogen ions in graphene layer, also increases electrical resistance and lowers the holes mobility. Consequently, an increase in the band gap of the layers is noticed. It is also important to mention here that plasma-based hydrogen functionalization requires certain order of frequencies i.e., kilohertz (kHz). Higher order of frequencies i.e., MHz etches the graphene layers (Nandana-palli et al. 2019).

Similar to hydrogenation, oxygen functionalization also imparts significant changes in electrical properties of graphene. Plasma-based oxygen functionalization is much appreciated approach owing to its simplicity and environment-friendly approach. For instance, (Liu et al. 2012a) functionalized graphene using controlled water-vapors supplied in the plasma chamber, operated at 100 W. In another approach graphene has been functionalized using oxygen/argon gas mixtures in

electron beam generated plasma. The oxygen functional groups increased the covalent bonds in graphene structure, and hence the surface-energy. Consequently, oxygen-functionalized graphene become reactive and very feasible for strong bonding between graphene and metals (Hopkins et al. 2012). CVD synthesized graphene has been modified in atmospheric pressure microwave plasma using O_2 gas. This approach of oxygen functionalization was quite useful to enhance the graphene semiconducting properties and chemical reactivity (Tincu et al. 2022).

Nitrogen functionalization using amine (NH_2) in plasma reactor has shown significant changes in graphene electrical and chemical properties, particularly used in biosensors. Such a functionalized graphene shows n-type conductive behavior. At lower plasma powers nitrogen functionalization occurs only at the edges of the graphene layers, whereas, at higher powers nitrogen bonds at complete basal plane. Consequently, higher powers functionalized graphene show a high decrease in the conductivity of the graphene (Baraket et al. 2012; Kato et al. 2011; Stine et al. 2012). Fluorination of graphene has shown great improvement in optical properties. For instance, one-sided fluorinated graphene has shown high optical transmittance and resistivity, which consisted of an optical band gap of 2.93 eV (Robinson et al. 2010).

(Alosaimi et al. 2022) demonstrated a graphene oxide modification technique using the atmospheric pressure plasma. The modification showed changes in the multiple properties such as chemistry, surface charge, electrical, wettability, thermal conductivity and the morphology of the graphene. These properties were obtained by exposing the graphene oxide to atmospheric pressure plasma. The process involves the reduction of graphene oxide into partially reduced-graphene oxide and reduced-graphene oxide. The procedure is advantageous because of its environmentally friendly nature and being very economical. Moreover, it can be performed on various substrates including metals, glass, semiconductors, Si, plastic etc.

The usage of microwave plasma to reduce the graphene oxide for the potential applications has been investigated. Polyethylene terephthalate (PET) coated with graphene oxide on its both sides has been successfully reduced to conductive reduced-graphene oxide. It was also shown that the addition of nitrogen gas into the reactor chamber converts the graphene oxide into a nitrogen-doped graphene oxide (Kalita et al. 2022).

8 Applications of graphene

8.1 Applications of PECVD grown graphene

8.1.1 Applications in supercapacitor

Owing to fast charge/discharge rate, high power density, and long cycle life in supercapacitors (pseudocapacitors and electric double-layer capacitors) have attracted great interest of scientists as a new energy storage device (Zhu et al. 2011; Purkait et al. 2017; Wang et al. 2009). Fast charge–discharge rate, long-life, high power and energy density are few characteristics which make supercapacitors different

and advanced from conventional capacitors. Supercapacitors are of two types, i.e. electric double-layer capacitors (EDLC) and pseudocapacitor. In EDLC electrical energy is stored by intercalating charges at electrolyte–electrode interface by making the double layer of charges. In this, charges are deposited physically due to the electrostatic attraction. Here graphene is used as an electrode material to store charges. Pseudocapacitor involve faradic reactions to store the electrical energy (Jiang and Liu 2019; Tomboc and Kim 2019; Choi et al. 2020). Graphene has been considered as a new alternative supercapacitor material due to its high conductivity and surface area. Moreover, vertical morphology of graphene is very suitable for the diffusion of ions (Seo et al. 2013b; Seo et al. 2014).

PECVD grown graphene grown on different substrates has also been investigated for supercapaciotrs applications using electrochemical studies. The graphene grown on Ni foam has shown excellent specific capacitance of 230 F/g at a scan rate of 10 mV/s. The results are shown in Fig. 9. The supercapacitor showed insignificant capacitance after 1500 cycles at high current density. It should also be noted that the capacitive behavior of graphene can be modified by controlling the plasma process parameters such as gas type and plasma power (Yang et al. 2013; Seo et al. 2013b).

(Miller et al. 2010) synthesized graphene from methane using RF-PECVD on Ni substrate. The as-synthesized graphene was utilized as an electrode in supercapacitor. In another study (Bo et al. 2012) synthesized graphene in PECVD for an electric double-layer capacitor. The binder-free electrode showed improved wettability and offered improved ion access. Resultantly, remarkable electrochemical properties were observed in aqueous and binder-free electrolytes.

8.1.2 Applications in sensors

Graphene materials are also widely used in variety of sensors owing to their remarkable sensitive properties (Yi et al. 2019; Wang et al. 2019). PECVD synthesized graphene was directly grown on Au/Si to form the heterojunction for its application in infrared photodetector. The deposited graphene formed strong van der Waals bond. Resultantly, a photo to dark ratio and responsivity was noted up to 2×10^4 and
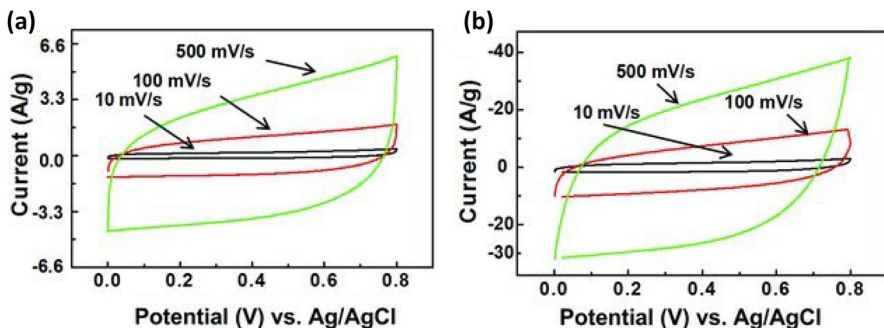

Fig. 9 Cyclic voltammetry (CV) curves of VGNS grown at **a** 40% and **b** 80% H_2 at varied scan rates (Seo et al. 2013b)

138 mA/W respectively (Liu et al. 2019). Comparing with CVD grown graphene, it was found that CVD graphene showed impurities and mismatching between graphene and Au/Si (Lupina et al. 2015). (Yang et al. 2019b) made graphene-based electrode for tunable and sensitive capacitive pressure sensor. The sensor showed fast response, low detection limit, tunable sensitivity, high sensitivity, stability and flexibility. This is a great example of graphene application in wearable health-monitoring devices. PECVD synthesized graphene-based sensors have also been used in various electrochemical sensors (Chen et al. 2020b; Li et al. 2016b; Huang et al. 2017b).

Wearable sensors with high sensitivity and stretchability are highly desirable. Graphene is now becoming an important part in wearable sensors and electronics. Compressing, stretching and flexibility are the important characteristics of wearable electronics. Graphene is combined with elastic materials in real applications to form wearable electronics. Robotics and wearable smart electronics are particularly using graphene as wearable sensor materials owing to graphene excellent properties of stretchability and sensitivity (Deng et al. 2019b; Zheng et al. 2021).

(Wu et al. 2018) developed a strain sensor made of graphene sandwiched between polydimethylsiloxane (PDMS). The sensor was non-corrosive to human sweat and insensitive to temperature. They found that the basal plane of vertical graphene is crucial in obtaining the high gauge factor in the strain sensor. Also, it was observed that the stretchability and sensitivity can be modified by altering the height of the vertical graphene.

In another stretchable sensors study (Yang et al. 2017) made electronic skin (E-skin) which showed very sensitive response to vocal cord vibration, joint and eye movement. The sensor demonstrated a gauge factor up to 65.9 with a 100% of maximum stretchability. The sensor is quite promising for its applications in wearable healthcare devices.

A temperature sensor based on graphene and polydimethylsiloxane (PDMS) was also developed. The sensor showed a temperature coefficient of 0.214 $°C^{-1}$, three times higher than that of conventional temperature sensors. It was due to the outstanding thermal sensitivity and stretchability of graphene. The sensor showed promising results for human body temperature sensing. Moreover, the recovery time of the sensor was quite efficient. It is shown in Fig. 10a (Yang et al. 2015). An electrochemical biosensor for lactate sensing has also been developed which showed wide linear range and low limit of detection. The cyclic voltametric response of detection is shown in Fig. 10b (Chen et al. 2017).

(Huang et al. 2018) fabricated parallelly aligned vertical graphene for wearable strain vector sensor. Due to the electrically anisotropic nature, the sensor was able to detect strain and amplitude of the strain vectors simultaneously. The human-sensor interface was investigated in real-time application for finger-joint movements.
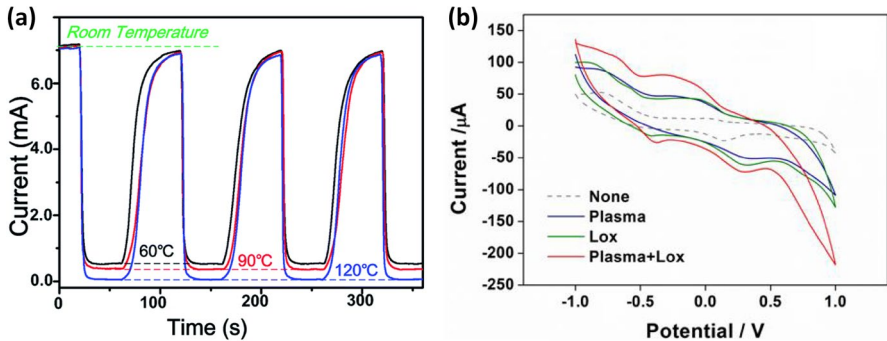
Fig. 10 **a** Wearable temperature sensor showing response/recovery time (Yang et al. 2015), **b** Cyclic voltametric response of different graphene-based sensors for lactate detection (Chen et al. 2017)

8.1.3 Applications in photovoltaic devices

A photovoltaic device converts sunlight energy into the electricity. Though much progresses have been made in photovoltaic devices, high production cost and low efficiency of the devices are still some of the challenges which require scientist's attention (Kim et al. 2011b). Benefitting from graphene's low sheet resistance and high transparency, graphene is now considered an ideal material to be used in current photovoltaic devices. For instance, graphene transparent electrodes have been used in organic photovoltaic devices (Liu et al. 2012b; Park et al. 2012a; Park et al. 2012b) and dye-sensitized solar cells (Das et al. 2011; Wang et al. 2008). Previously used CVD techniques require the transferring of the synthesized graphene on required substrates for photovoltaic devices. The transferring process produces cracks or wrinkles in the graphene, which affect the quality of the graphene. PECVD has the ability to directly synthesize graphene on variety of substrates and which at the same time has low sheet resistance and high transparency (Yang et al. 2012).

Carbon-based heterostructure junctions are now widely appreciated in solar cells. P-N and Schottky junction are some examples of it. Graphene Schottky junction is more valued due to its excellent charge separation efficiency and large built-in field (Chen et al. 2015c; Li et al. 2010). The power conversion efficiency in graphene is still need scientist's attentions. An example of that is the fabrication of graphene-graphitic film on silicon substrate. However, this graphene/silicon schottky junction solar cell showed poor efficiency of 0.078%.

PECVD fabricated graphene nanowalls are another example of graphene-based materials, employed in solar cells. Their use include as a counter electrode in dye-sensitized solar cells (McClure et al. 2012). The dye-sensitized solar cells made of as-synthesized and hydrogen plasma treated graphene nanowalls showed improved power conversion efficiency. The power conversion efficiency in plasma treated solar cell was higher than as-synthesized graphene. It is attributed to the reduction in sheet resistance of graphene material (Jung et al. 2014). The power conversion efficiency can be increased even more by fabricating graphene nanowalls directly on silicon substrate. For instance, (Liu et al. 2015) reported 5.1% of power conversion

efficiency of such a heterojunction material. It was attributed to the high surface area of vertical graphene nanowalls.

(Bayram et al. 2020) synthesized graphene/polyaniline nanocomposite using the PECVD setup for the dye-sensitized solar cell application. Graphene/polyaniline nanocomposite was used as a counter electrode. Nanocomposite was prepared in multi-steps. It includes single and multilayer graphene films fabrication on fluorine-doped tin oxide substrate. Subsequently, polyaniline films were produced on graphene films. The dye-sensitized solar cell comprised of N719 dye, iodolyte liquid electrolyte, titanium dioxide (TiO_2) nanotube photoanode, and graphene/PANI nanocomposite. It is shown in Fig. 11a. Current–voltage characterization given in Fig. 11b showed that photo-conversion efficiency varied between 0.56 and 1.36% depending upon the number of layers of graphene. The photovoltaic performance of dye-sensitized solar cell was recorded as 1.1%.
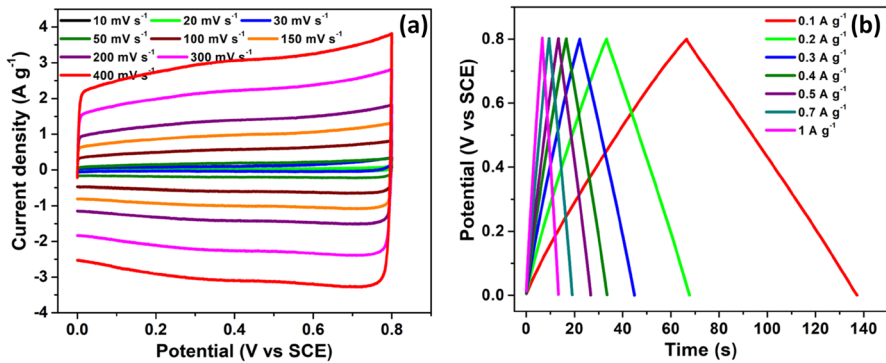
8.2 Applications of atmospheric pressure microwave plasma-synthesized graphene

8.2.1 Applications in supercapacitor

Nitrogen-doped graphene synthesized in atmospheric pressure plasma was used as an electrode in supercapacitor application. Electrochemical methods i.e., cyclic voltammetry, electrochemical impedance spectroscopy, and galvanostatic charge–discharge were used for this purpose. As expected from a charge storing material, N-graphene showed perfect rectangular structure. It is shown in Fig. 12a. The cathodic and anodic current responses showed an increase with the increase of scan rate, and a rectangular shape was observed even at 400 mV/s scan rate. Galvanostatic charge–discharge measurement were conducted at current densities ranging between 0.1 and 1 A/g. It is shown in Fig. 12b. The results showed linear charge and discharge behavior at all current densities which prove the electric double-layer capacitance behavior. Moreover, specific capacitance of
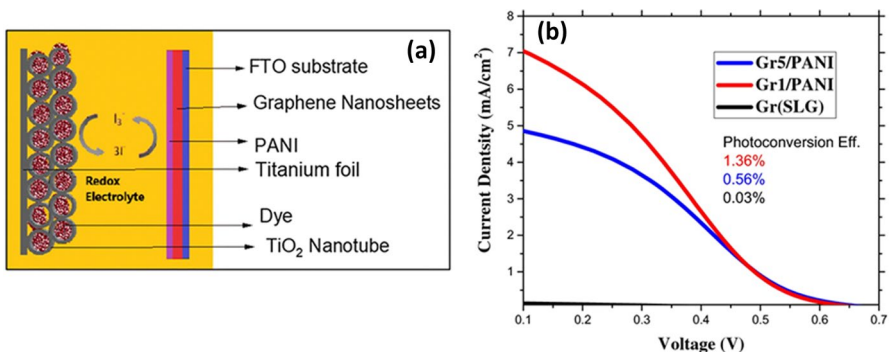
Fig. 11 **a** Dye-sensitized solar cell configuration, **b** J-V curves of graphene/polyaniline curves (Bayram et al. 2020)

Fig. 12 **a** Cyclic voltammograms of N-doped graphene at various scan rates, **b** Galvanic charge–discharge at various current densities (Bundaleska et al. 2018b)

8.87 F/g was attained at 0.1 A/g current density. The specific capacitance retained its value even at increased amount of currents (Bundaleska et al. 2018b).

8.2.2 Applications in sensors

The atmospheric pressure microwave plasma-synthesized nitrogen-doped graphene oxide has also shown remarkable results in electrochemical sensing of oxalic acid (Zafar et al. 2022a). Oxalic acid could have adverse effects on human health if consumed excessively. Thus, it is very important to detect oxalic acid in foods. Ag-Nps loaded nitrogen-doped graphene oxide drop-casted on glassy carbon electrode was used as a working electrode in this study. The electrode was used for oxalic acid detection in a phosphate buffer solution. Compared with bare or nitrogen-doped graphene oxide showed prominent peak current in cyclic voltammetry measurements. The cyclic voltammetry results are shown in Fig. 13. Furthermore, characterized through chronoamperometry, the electrochemical sensor showed a lower limit of detection and a wide linear range i.e., 2 µM

Fig. 13 Cyclic voltmmograms of modified working electrodes for oxalic acid detection in a phosphate buffer solution (Zafar et al. 2022a)
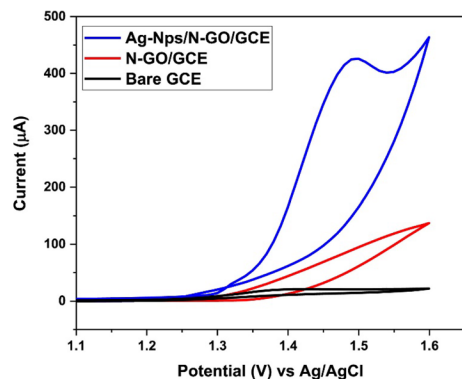
and 10–300 μM respectively. Attributed to the anti-fouling properties of nitrogen-doped graphene oxide, the proposed sensor demonstrated excellent stability and repeatability results. Graphene synthesized using the microwave plasma has proven its excellency in herbicide detection. A wide linear range and a remarkable limit of detection was noted for diuron detection.

8.2.3 Application in water desalination

Nitrogen-doped graphene oxide, synthesized in atmospheric pressure microwave plasma from a single source i.e., aniline was used in a demonstration application of desalination. A lab scale developed desalination system was used for this purpose. Commercially available polyamide membrane was used in this application. The membrane was coated with nitrogen-doped graphene oxide using the drop-casting method. It is shown schematically in Fig. 14a. The nitrogen-doped graphene oxide coating did not affect much hydrophilicity of the membrane, shown through water contact angle in Fig. 14b, c. However, nitrogen-doped graphene oxide coating improved the flux recovery ratio (Fig. 14d), which can be attributed to the excellent anti-scaling properties of the nitrogen-doped graphene oxide material (Zafar et al. 2022b).

8.2.4 Applications in catalysis and battery

The dispersion of nanoparticles on base materials is critical for catalysis applications. It is highly desired that the catalytic nanoparticles should have high surface area, and avoid any aggregation (Zhu and Xu 2016; Gao et al. 2019). Graphene for
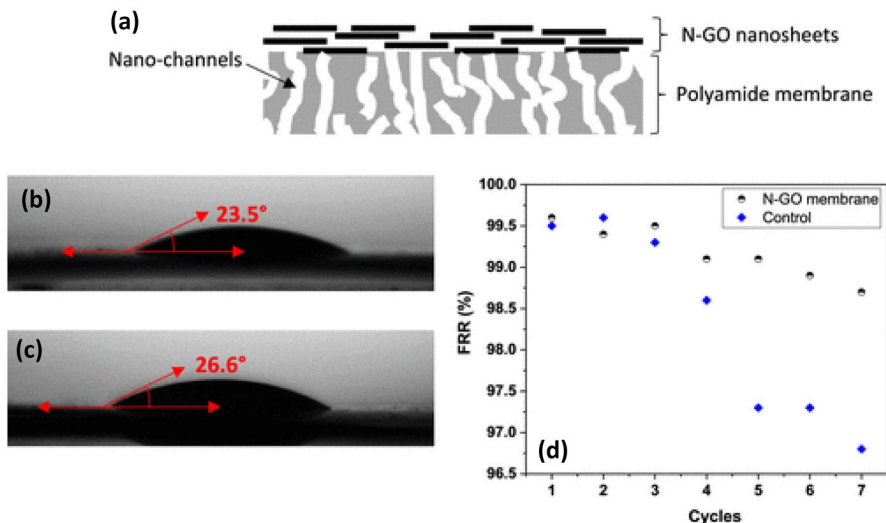
Fig. 14 **a** Schematic demonstration of the nitrogen-doped graphene oxide -coated-polyamide membrane, **b** water contact angle of the polyamide and **c** nitrogen-doped graphene oxide-coated-polyamide membranes, and **d** flux recovery ratio after number of cycles of water filtration (Zafar et al. 2022b)

dispersion of nanoparticles can play an important role. In a study, gold nanoparticles of varying diameters were spread on graphene synthesized through atmospheric pressure microwave plasma. The study revealed that the small sizes nanoparticles i.e. less than 10 nm tend to locate on the edges of the graphene nsnosheets, and avoided aggregations. It means, nanoparticles less than 10 nm dispersed on graphene nanosheets can be useful in catalysis applications (Jeon and Lee 2011).

In another study by (Jo et al. 2016) Pt/graphene nanocomposite was prepared in microwave plasma. The nanocomposite was investigated for its application in electrocatalysis. Investigated through cyclic voltammetry, the Pt/graphene nanocomposite showed excellent electrocatalytic activity for the methanol oxidation. Compared with other Pt composites with carbon and graphene, this study revealed that the electrocatalytic results were superior. It can be attributed to the high dispersion of Pt on graphene, and graphene's high electrocatalytic properties.

Graphene nanosheets synthesized in atmospheric pressure microwave plasma havv also been used for its application in battery. For instance, graphene nanosheets and Si nanocomposite was used in Li-ion battery. Compared with other reported Si composites, graphene/Si nanocomposite anode outperformed all those and showed superior Coulomb efficiency and longer stability (Münzer et al. 2018; Tan et al. 2103; Xu et al. 2014).

9 Conclusion and future outlook

The production of superior quality graphene in a fast and efficient way is one of the merits of Plasma-based synthesis method. PECVD synthesis of graphene is a widely adopted bottom-down approach capable of producing monolayer to few layers graphene. In comparison to top-down methods where graphite is the main resource for graphene, PECVD is a versatile approach as it can synthesize graphene from a diverse range of precursors, such as natural gas, botanical hydrocarbons, food products, polymers, wastes, etc. Furthermore, shorter processing time and absence of additional chemical requirements are two more benefits of PECVD. However, the need for high vacuum and low chamber pressure makes the process tiresome. In addition, the requisite for a substrate and the subsequent transfer of graphene for further applications are some issues needed to be addressed in this procedure. Moreover, the biggest challenge for this technique is the scalable preparation of graphene. Therefore, to convert this system into an industrial-scale process, more attention must be given to the scalable synthesis of graphene.

Atmospheric pressure microwave plasma synthesis of graphene is another state-of-the-art technique to synthesize graphene. This method certainly has some advantages over PECVD as it does not require high vacuum or low chamber pressure conditions to produce graphene. In contrast to PECVD, it offers scalable graphene; however, the amount synthesized is still not adequate for large-scale production. Besides, the process is generally reliant on the usage of non-sustainable precursors. Thus, it is pivotal to substitute these unrenewable precursors with environmental-friendly and sustainable resources. It is extremely critical to demonstrate the real application of any material; however, the practical usage of graphene synthesized

through atmospheric pressure microwave plasma has scarcely been reported. Therefore, it is highly crucial to demonstrate the potential applications of graphene produced through this method.

Furthermore, a theoretical study of the complex growth environment of the atmospheric pressure plasma, as well as PECVD, should be carried out for a complete understanding of the process. The above-mentioned processes have used only a continuous mode of plasma. Varying the plasma source to pulse mode may vary the chamber environment substantially. Thus, its effects on the synthesis should be investigated. Remarkable work on the synthesis of nanocomposite of graphene with other nanomaterials using wet chemical methods is widely reported. However, the synthesis in a dry and chemical-free environment of plasma still lacks. Scale-up of the laboratory-scale reaction chambers is essential for the industrialization of the technologies. Although, applications of plasma-synthesized graphene in electrochemical sensors, batteries, supercapacitors, membranes, etc. have been demonstrated at a lab scale. It is also very important to showcase its broad use in potential future applications such as transistors, semiconductors, bendable phones, medical science, wearable electronics and sensors, metals recovery, crop protection and growth, etc.

Declarations

Conflict of interest The authors claims that they have no conflicts of interest.

References

T. Aissou, N. Braidy, J. Veilleux, A new one-step deposition approach of graphene nanoflakes coating using a radio frequency plasma: synthesis, characterization and tribological behaviour. Tribol. Int. **167**, 107406 (2022)

S. Alancherry et al. *Fabrication of nano-onion-structured graphene films from citrus sinensis extract and their wetting and sensing characteristics.* (ACS Applied Materials & Interfaces, 2020)

M. Aliofkhazraei. *Advances in graphene science.* (BoD–Books on Demand, 2013)

A. Al-Jumaili et al., Review on the antimicrobial properties of carbon nanostructures. Materials **10**(9), 1066 (2017)

A. Al-Jumaili et al., Bactericidal vertically aligned graphene networks derived from renewable precursor. Carbon. Trends. **7**, 100157 (2022)

B.L. Allen, P.D. Kichambare, A. Star, Carbon nanotube field-effect-transistor-based biosensors. Adv. Mater. **19**(11), 1439–1451 (2007)

M.J. Allen, V.C. Tung, R.B. Kaner, Honeycomb carbon: a review of graphene. Chem. Rev. **110**(1), 132–145 (2009)

F.K. Alosaimi et al., Graphene-based multifunctional surface and structure gradients engineered by atmospheric plasma. Appl. Mater. Today **27**, 101486 (2022)

P. Avouris, Z. Chen, V. Perebeinos, Carbon-based electronics. Nat. Nanotechnol. **2**(10), 605–615 (2007)

K. Awasthi et al., Large scale synthesis of bundles of aligned carbon nanotubes using a natural precursor: turpentine oil. J. Exp. Nanosci. **5**(6), 498–508 (2010)

S.N. Baker, G.A. Baker, Luminescent carbon nanodots: emergent nanolights. Angew. Chem. Int. Ed. **49**(38), 6726–6744 (2010)

M. Baraket et al., Aminated graphene for DNA attachment produced via plasma functionalization. Appl. Phys. Lett. **100**(23), 233123 (2012)

O. Bayram et al., Graphene/polyaniline nanocomposite as platinum-free counter electrode material for dye-sensitized solar cell: its fabrication and photovoltaic performance. J. Mater. Sci.: Mater. Electron. **31**(13), 10288–10297 (2020)

E. Bertin et al., Durability study of platinum nanoparticles supported on gas-phase synthesized graphene in oxygen reduction reaction conditions. Appl. Surf. Sci. **467**, 1181–1186 (2019)

M.S.A. Bhuyan et al., Synthesis of graphene. Int. Nano. Lett. **6**(2), 65–83 (2016)

A. Biswas et al., Advances in top–down and bottom–up surface nanofabrication: techniques, applications & future prospects. Adv. Coll. Interface. Sci. **170**(1), 2–27 (2012)

Z. Bo et al., One-step fabrication and capacitive behavior of electrochemical double layer capacitor electrodes using vertically-oriented graphene directly grown on metal. Carbon **50**(12), 4379–4387 (2012)

Z. Bo et al., Plasma-enhanced chemical vapor deposition synthesis of vertically oriented graphene nanosheets. Nanoscale **5**(12), 5180–5204 (2013)

A.R. Botello-Méndez et al., One-dimensional extended lines of divacancy defects in graphene. Nanoscale **3**(7), 2868–2872 (2011)

D. Boyd et al., Single-step deposition of high-mobility graphene at reduced temperatures. Nat. Commun. **6**, 6620 (2015)

N. Bundaleska et al., Microwave plasma enabled synthesis of free standing carbon nanostructures at atmospheric pressure conditions. Phys. Chem. Chem. Phys. **20**(20), 13810–13824 (2018a)

N. Bundaleska et al., Large-scale synthesis of free-standing N-doped graphene using microwave plasma. Sci. Rep. **8**(1), 1–11 (2018b)

A. Casanova et al., Optimizing high-quality graphene nanoflakes production through organic (bio)-precursor plasma decomposition. Fuel Process. Technol. **212**, 106630 (2021)

S.M. Chen et al., Hydrogen-free synthesis of graphene-graphitic films directly on Si substrate by plasma enhanced chemical vapor deposition. J. Mater. Sci-Mater. Electronics. **26**(3), 1485–1493 (2015a)

J. Chen, Z. Bo, G. Lu, The properties of vertically-oriented graphene, in *Vertically-oriented graphene*. (Springer, Berlin, 2015b), pp.11–18

S. Chen et al., Hydrogen-free synthesis of graphene–graphitic films directly on Si substrate by plasma enhanced chemical vapor deposition. J. Mater. Sci.: Mater. Electron. **26**(3), 1485–1493 (2015c)

Q. Chen et al., Flexible electrochemical biosensors based on graphene nanowalls for the real-time measurement of lactate. Nanotechnology **28**(31), 315501 (2017)

C. Chen et al., Understanding the effect of hydroxyl/epoxy group on water desalination through lamellar graphene oxide membranes via molecular dynamics simulation. Desalination **491**, 114560 (2020a)

F. Chen et al., β-cyclodextrin-immobilized Ni/graphene electrode for electrochemical enantiorecognition of phenylalanine. Materials **13**(3), 777 (2020b)

W.H. Chiang et al., Microplasmas for advanced materials and devices. Adv. Mater. **32**(18), 1905508 (2020)

C. Choi et al., Achieving high energy density and high power density with pseudocapacitive materials. Nat. Rev. Mater. **5**(1), 5–19 (2020)

S. Das et al., Amplifying charge-transfer characteristics of graphene for triiodide reduction in dye-sensitized solar cells. Adv. Func. Mater. **21**(19), 3729–3736 (2011)

A. Dato, Graphene synthesized in atmospheric plasmas—a review. J. Mater. Res. **34**(1), 214–230 (2019)

A. Dato, M. Frenklach, Substrate-free microwave synthesis of graphene: experimental conditions and hydrocarbon precursors. New J. Phys. **12**(12), 125013 (2010)

A. Dato et al., Substrate-free gas-phase synthesis of graphene sheets. Nano Lett. **8**(7), 2012–2016 (2008)

A. Dato et al., Clean and highly ordered graphene synthesized in the gas phase. Chem. Commun. **40**, 6095–6097 (2009)

B. Deng, Z.F. Liu, H.L. Peng, Toward mass production of CVD graphene films. Adv. Mater. **31**(9), 1800996 (2019a)

C. Deng et al., Ultrasensitive and highly stretchable multifunctional strain sensors with timbre-recognition ability based on vertical graphene. Adv. Func. Mater. **29**(51), 1907151 (2019b)

D.R. Dreyer et al., The chemistry of graphene oxide. Chem. Soc. Rev. **39**(1), 228–240 (2010)

D.C. Elias et al., Control of graphene's properties by reversible hydrogenation: evidence for graphane. Science **323**(5914), 610–613 (2009)

P. Fortugno et al., Synthesis of freestanding few-layer graphene in microwave plasma: the role of oxygen. Carbon **186**, 560–573 (2022)

M. Fronczak et al., Continuous and catalyst free synthesis of graphene sheets in thermal plasma jet. Chem. Eng. J. **322**, 385–396 (2017)

M. Fronczak et al., Facile and continuous synthesis of graphene nanoflakes in RF thermal plasma. Carbon **193**, 51–67 (2022)

H. Gao et al., Synthesis of S-doped graphene by liquid precursor. Nanotechnology **23**(27), 275605 (2012)

X. Gao et al., Carbon-dot-based ratiometric fluorescent probe for imaging and biosensing of superoxide anion in live cells. Anal. Chem. **86**(14), 7071–7078 (2014)

Y. Gao et al., A Robust Au/ZnCr2O4 catalyst with highly dispersed gold nanoparticles for gas-phase selective oxidation of cyclohexanol to cyclohexanone. ACS Catal. **9**(12), 11104–11115 (2019)

A.K. Geim, Graphene: status and prospects. Science **324**(5934), 1530–1534 (2009)

S. Ghosh et al., Process-specific mechanisms of vertically oriented graphene growth in plasmas. Beilstein J. Nanotechnol. **8**(1), 1658–1670 (2017)

A. Guermoune et al., Chemical vapor deposition synthesis of graphene on copper with methanol, ethanol, and propanol precursors. Carbon **49**(13), 4204–4210 (2011)

M.G. Hahm et al., Carbon nanotube–nanocup hybrid structures for high power supercapacitor applications. Nano Lett. **12**(11), 5616–5621 (2012)

Y. Hancock, The 2010 Nobel Prize in physics—ground-breaking experiments on graphene. J. Phys. D Appl. Phys. **44**(47), 473001 (2011)

J. Hass, W. De Heer, E. Conrad, The growth and morphology of epitaxial multilayer graphene. J. Phys.: Condens. Matter **20**(32), 323202 (2008)

R. Hatakeyama, Nanocarbon materials fabricated using plasmas. Rev. Modern. Plasma. Phys. **1**(1), 7 (2017)

U.S. Heo et al., A facile synthesis of anatase TiO2-Graphene nanocomposites using plasma and heat treatment. Appl. Surf. Sci. **474**, 118–126 (2019)

M. Hiramatsu et al., Fabrication of graphene-based films using microwave-plasma-enhanced chemical vapor deposition. Japanese. J. Appl. Phys. **52**(1), 01AK04 (2013)

P.E. Hopkins et al., Manipulating thermal conductance at metal–graphene contacts via chemical functionalization. Nano Lett. **12**(2), 590–595 (2012)

S. Huang et al., Graphene plasmonics: physics and potential applications. Nanophotonics **6**(6), 1191–1204 (2017a)

B. Huang et al., A free-standing electrochemical sensor based on graphene foam-carbon nanotube composite coupled with gold nanoparticles and its sensing application for electrochemical determination of dopamine and uric acid. J. Electroanal. Chem. **801**, 129–134 (2017b)

S. Huang et al., Stretchable strain vector sensor based on parallelly aligned vertical graphene. ACS Appl. Mater. Interfaces. **11**(1), 1294–1302 (2018)

S. Iijima, Helical microtubules of graphitic carbon. Nature **354**(6348), 56–58 (1991)

A.A. Iqbal et al., Graphene-based nanocomposites and their fabrication, mechanical properties and applications. Materialia **12**, 100815 (2020)

M.V. Jacob et al., Catalyst-free plasma enhanced growth of graphene from sustainable sources. Nano Lett. **15**(9), 5702–5708 (2015)

A. Jagodar et al., Nitrogen incorporation in graphene nanowalls via plasma processes: experiments and simulations. Appl. Surf. Sci. **591**, 153165 (2022)

K.-J. Jeon, Z. Lee, Size-dependent interaction of Au nanoparticles and graphene sheet. Chem. Commun. **47**(12), 3610–3612 (2011)

Y. Jiang, J. Liu, Definitions of pseudocapacitive materials: a brief review. Energy. Env. Mater. **2**(1), 30–37 (2019)

Q. Jiangying et al., Highly atom-economic synthesis of graphene/Mn 3 O 4 hybrid composites for electrochemical supercapacitors. Nanoscale **5**(7), 2999–3005 (2013)

E.H. Jo et al., One-step synthesis of Pt/Graphene composites from Pt acid dissolved ethanol via microwave plasma spray pyrolysis. Sci. Rep. **6**(1), 33236 (2016)

Y.H. Jung, W.S. Choi, B. Hong, Post-plasma treatment of a carbon nanowall for use as a counter electrode in a dye-sensitized solar cell. J. Korean Phys. Soc. **65**(3), 291–296 (2014)

G. Kalita, K. Wakita, M. Umeno, Low temperature growth of graphene film by microwave assisted surface wave plasma CVD for transparent electrode application. RSC Adv. **2**(7), 2815–2820 (2012)

G. Kalita, B.P. Jaisi, M. Umeno, Effective reduction and doping of graphene oxide films at near-room temperature by microwave-excited surface-wave plasma process. Diam. Relat. Mater. **126**, 109066 (2022)

T. Kato et al., Room-temperature edge functionalization and doping of graphene by mild plasma. Small **7**(5), 574–577 (2011)

R. Kato et al., High growth rate chemical vapor deposition of graphene under low pressure by RF plasma assistance. Carbon **96**, 1008–1013 (2016)

D.R. Kauffman, A. Star, Carbon nanotube gas and vapor sensors. Angew. Chem. Int. Ed. **47**(35), 6550–6570 (2008)

J. Kim et al., Fabrication of graphene flakes composed of multi-layer graphene sheets using a thermal plasma jet system. Nanotechnology **21**(9), 095601 (2010)

Y. Kim et al., Low-temperature synthesis of graphene on nickel foil by microwave plasma chemical vapor deposition. Appl. Phys. Lett. **98**(26), 263106 (2011a)

J.P. Kim et al., Numerical analysis on the thermal characteristics of photovoltaic module with ambient temperature variation. Sol. Energy Mater. Sol. Cells **95**(1), 404–407 (2011b)

D.-W. Kim et al., One-step synthesis of TiC/multilayer graphene composite by thermal plasma. Curr. Appl. Phys. **18**(5), 551–558 (2018)

W. Krätschmer, L. Lamb, K. Fostiropoulos, D.R. Huffman, Nature **347**, 354 (1990)

A. Kumar et al., Nitrogen-doped graphene by microwave plasma chemical vapor deposition. Thin Solid Films **528**, 269–273 (2013)

R. Kumar et al., Clean and efficient synthesis of graphene nanosheets and rectangular aligned-carbon nanotubes bundles using green botanical hydrocarbon precursor: sesame oil. Sci. Adv. Mater. **6**(1), 76–83 (2014)

R. Kumar, R.K. Singh, D.P. Singh, Natural and waste hydrocarbon precursors for the synthesis of carbon based nanomaterials: graphene and CNTs. Renew. Sustain. Energy Rev. **58**, 976–1006 (2016)

M.W. Lee et al., Fabrication of dispersible graphene flakes using thermal plasma jet and their thin films for solar cells. Carbon **106**, 48–55 (2016)

H.C. Lee et al., Review of the synthesis, transfer, characterization and growth mechanisms of single and multilayer graphene. RSC Adv. **7**(26), 15644–15693 (2017)

X.J. Lee et al., Review on graphene and its derivatives: Synthesis methods and potential industrial implementation. J. Taiwan Inst. Chem. Eng. **98**, 163–180 (2019)

J.H. Lehman et al., Evaluating the characteristics of multiwall carbon nanotubes. Carbon **49**(8), 2581–2602 (2011)

X. Li et al., Graphene-on-silicon Schottky junction solar cells. Adv. Mater. **22**(25), 2743–2748 (2010)

M. Li et al., Controllable synthesis of graphene by plasma-enhanced chemical vapor deposition and its related applications. Adv Sci (weinh) **3**(11), 1600003 (2016a)

Y. Li et al., Fabrication of ultra-sensitive and selective dopamine electrochemical sensor based on molecularly imprinted polymer modified graphene@ carbon nanotube foam. Electrochem. Commun. **64**, 42–45 (2016b)

C. Li et al., A facile and green preparation of reduced graphene oxide using eucalyptus leaf extract. Appl. Surf. Sci. **422**, 469–474 (2017)

X.-Q. Li et al., Preparation of isolated semiconducting single-wall carbon nanotubes by oxygen-assisted floating catalyst chemical vapor deposition. Chem. Eng. J. **450**, 137861 (2022)

H. Liu, T. Ye, C. Mao, Fluorescent carbon nanoparticles derived from candle soot. Angew. Chem. **119**(34), 6593–6595 (2007)

L. Liu et al., Controlled oxidative functionalization of monolayer graphene by water-vapor plasma etching. Carbon **50**(8), 3039–3044 (2012a)

Z. Liu et al., Package-free flexible organic solar cells with graphene top electrodes the application of highly doped single-layer graphene as the top electrodes of semitransparent organic solar cells. ACS Nano **6**, 810–818 (2012b)

J. Liu et al., Direct growth of graphene nanowalls on the crystalline silicon for solar cells. Appl. Phys. Lett. **106**(4), 043904 (2015)

H. Liu et al., Carbon nanostructures in biology and medicine. J. Mater. Chem B. **5**(32), 6437–6450 (2017)

X. Liu et al., Infrared photodetector based on the photothermionic effect of graphene-nanowall/silicon heterojunction. ACS Appl. Mater. Interfaces. **11**(19), 17663–17669 (2019)

M. Lotya et al., Liquid phase production of graphene by exfoliation of graphite in surfactant/water solutions. J. Am. Chem. Soc. **131**(10), 3611–3620 (2009)

G. Lupina et al., Residual metallic contamination of transferred chemical vapor deposited graphene. ACS Nano **9**(5), 4776–4785 (2015)

C. Ma, H. Yu, K. Yu, Plasma-enhanced chemical vapor deposition of graphene optimized by pressure. Mater. Res. Express. **6**, 105605 (2019a)

Y. Ma et al., Experimental investigation on vertically oriented graphene grown in a plasma-enhanced chemical vapor deposition process. ACS Appl. Mater. Interfaces. **11**(10), 10237–10243 (2019b)

A. Malesevic et al., Synthesis of few-layer graphene via microwave plasma-enhanced chemical vapour deposition. Nanotechnology **19**(30), 305604 (2008)

H.Y. Mao et al., Graphene: promises, facts, opportunities, and challenges in nanomedicine. Chem. Rev. **113**(5), 3407–3424 (2013)

A. Martinez, K. Fuse, S. Yamashita, Mechanical exfoliation of graphene for the passive mode-locking of fiber lasers. Appl. Phys. Lett. **99**(12), 121107 (2011)

J.P. McClure et al., Oxygen reduction on metal-free nitrogen-doped carbon nanowall electrodes. J. Electrochem. Soc. **159**(11), F733 (2012)

C. Melero et al., Scalable graphene production from ethanol decomposition by microwave argon plasma torch. Plasma. Phys. Controll. Fusion. **60**(1), 014009 (2017)

J.R. Miller, R. Outlaw, B. Holloway, Graphene double-layer capacitor with ac line-filtering performance. Science **329**(5999), 1637–1639 (2010)

R. Muñoz, C. Gómez-Aleixandre, Review of CVD synthesis of graphene. Chem. Vapor. Depos. **19**, 297–322 (2013)

A. Münzer et al., All gas-phase synthesis of graphene: characterization and its utilization for silicon-based lithium-ion batteries. Electrochim. Acta **272**, 52–59 (2018)

K. Nakahara et al., Enhanced mechanical properties of epoxy-matrix nanocomposites reinforced with graphene synthesized in atmospheric plasmas. Plasma Processes Polym. **17**(5), 1900244 (2020)

K.R. Nandanapalli, D. Mudusu, S. Lee, Functionalization of graphene layers and advancements in device applications. Carbon **152**, 954–985 (2019)

S. Nasir et al., Oil palm waste-based precursors as a renewable and economical carbon sources for the preparation of reduced graphene oxide from graphene oxide. Nanomaterials **7**(7), 182 (2017)

S. Niyogi et al., Chemistry of single-walled carbon nanotubes. Acc. Chem. Res. **35**(12), 1105–1113 (2002)

K.S. Novoselov et al., A roadmap for graphene. Nature **490**(7419), 192–200 (2012)

K. Ostrikov, E. Neyts, M. Meyyappan, Plasma nanoscience: from nano-solids in plasmas to nano-plasmas in solids. Adv. Phys. **62**(2), 113–224 (2013)

S. Park et al., Electron microscopy analyses of natural and highly oriented pyrolytic graphites and the mechanically exfoliated graphenes produced from them. Carbon **48**(3), 797–804 (2010)

H. Park et al., Graphene as transparent conducting electrodes in organic photovoltaics: studies in graphene morphology, hole transporting layers, and counter electrodes. Nano Lett. **12**(1), 133–140 (2012a)

H. Park et al., Organic solar cells with graphene electrodes and vapor printed poly (3, 4-ethylenedioxythiophene) as the hole transporting layers. ACS Nano **6**(7), 6370–6377 (2012b)

J. Peng et al., Graphene quantum dots derived from carbon fibers. Nano Lett. **12**(2), 844–849 (2012)

K.-J. Peng et al., Hydrogen-free PECVD growth of few-layer graphene on an ultra-thin nickel film at the threshold dissolution temperature. J. Mater. Chem C. **1**(24), 3862–3870 (2013)

T. Pimklang, A. Watthanaphanit, P. Pakawatpanurut, Novel green synthesis of graphene oxide-manganese dioxide using solution plasma process for energy storage. Chem. Eng. J. **442**, 136244 (2022)

T. Purkait et al., Large area few-layer graphene with scalable preparation from waste biomass for high-performance supercapacitor. Sci. Rep. **7**(1), 1–14 (2017)

C.R.B. Purna et al., Low temperature growth of carbon nanostructures by radio frequency-plasma enhanced chemical vapor deposition (low temperature growth of carbon nanostructures by RF-PECVD). Fuller. Nanotubes. Carbon. Nanostruct. **17**(6), 625–635 (2009)

J. Qi et al., Relatively low temperature synthesis of graphene by radio frequency plasma enhanced chemical vapor deposition. Appl. Surf. Sci. **257**(15), 6531–6534 (2011)

M. Qi et al., Hydrogen kinetics on scalable graphene growth by atmospheric pressure chemical vapor deposition with acetylene. J. Phys. Chem C. **117**(27), 14348–14353 (2013)

R. Rincón et al., Synthesis of multi-layer graphene and multi-wall carbon nanotubes from direct decomposition of ethanol by microwave plasma without using metal catalysts. Plasma. Sources. Sci. Technol. **24**(3), 032005 (2015)

J.T. Robinson et al., Properties of fluorinated graphene films. Nano Lett. **10**(8), 3001–3005 (2010)

S. Sahoo et al., A review on supercapacitors based on plasma enhanced chemical vapor deposited vertical graphene arrays. J. Energy. Storage. **53**, 105212 (2022)

D.H. Seo et al., Plasma break-down and Re-build: Same functional vertical graphenes from diverse natural precursors. Adv. Mater. **25**(39), 5638–5642 (2013a)

D.H. Seo et al., Structure-controlled, vertical graphene-based, binder-free electrodes from plasma-reformed butter enhance supercapacitor performance. Adv. Energy Mater. **3**(10), 1316–1323 (2013b)

D.H. Seo et al., Synergistic fusion of vertical graphene nanosheets and carbon nanotubes for high-performance supercapacitor electrodes. Chemsuschem **7**(8), 2317–2324 (2014)

D.H. Seo et al., Single-step ambient-air synthesis of graphene from renewable precursors as electrochemical genosensor. Nat. Commun. **8**, 14217 (2017)

S. Sharma et al., Influence of gas composition on the formation of graphene domain synthesized from camphor. Mater. Lett. **93**, 258–262 (2013)

C.J. Shearer et al., Accurate thickness measurement of graphene. Nanotechnology **27**(12), 125704 (2016)

B. Shen et al., Influence of different buffer gases on synthesis of few-layered graphene by arc discharge method. Appl. Surf. Sci. **258**(10), 4523–4531 (2012)

Shunhong, Z. et al. Penta-graphene: a new carbon allotrope. Радиоэлектроника. Наносистемы. Информационные технологии, 2015. **7**(2)

M. Singh et al., Effect of hydrogen concentration on graphene synthesis using microwave-driven plasma-mediated methane cracking. Carbon **143**, 802–813 (2019a)

M. Singh, H.S. Jha, P. Agarwal, Synthesis of vertically aligned carbon nanoflakes by hot-wire chemical vapor deposition: Influence of process pressure and different substrates. Thin Solid Films **678**, 26–31 (2019b)

M. Somekh, E. Shawat, G.D. Nessim, Fully reproducible, low-temperature synthesis of high-quality, few-layer graphene on nickel via preheating of gas precursors using atmospheric pressure chemical vapor deposition. J. Mater. Chem a. **2**(46), 19750–19758 (2014)

X. Song et al., Direct versatile PECVD growth of graphene nanowalls on multiple substrates. Mater. Lett. **137**, 25–28 (2014)

R. Stine et al., High-density amine-terminated monolayers formed on fluorinated CVD-grown graphene. Langmuir **28**(21), 7957–7961 (2012)

S.S. Sukumaran et al., Raman and scanning tunneling spectroscopic investigations on graphene-silver nanocomposites. J. Sci.: Adv. Mater. Devices. **3**(3), 353–358 (2018)

Y.-P. Sun et al., Quantum-sized carbon dots for bright and colorful photoluminescence. J. Am. Chem. Soc. **128**(24), 7756–7757 (2006)

D.H. Tan et al. *Carbon free high loading silicon anodes enabled by sulfide solid electrolytes for robust all solid-state batteries.* arXiv preprint arXiv:2103.04230, (2021)

Y. Tanaka et al., High rate synthesis of graphene-encapsulated silicon nanoparticles using pulse-modulated induction thermal plasmas with intermittent feedstock feeding. Japanese J. Appl. Phys. **59**(SH), SHHE07 (2020)

E. Tatarova et al., Microwave plasma based single step method for free standing graphene synthesis at atmospheric conditions. Appl. Phys. Lett. **103**(13), 134101 (2013)

E. Tatarova et al., Microwave plasmas applied for the synthesis of free standing graphene sheets. J. Phys. D Appl. Phys. **47**(38), 385501 (2014)

E. Tatarova et al., Microwave plasmas applied for synthesis of free-standing carbon nanostructures at atmospheric pressure conditions. J. Magnetohydrodynamics. Plasma. Res. **21**(2), 185 (2016)

E. Tatarova et al., Towards large-scale in free-standing graphene and N-graphene sheets. Sci. Rep. **7**(1), 1–16 (2017)

T.-O. Terasawa, K. Saiki, Growth of graphene on Cu by plasma enhanced chemical vapor deposition. Carbon **50**(3), 869–874 (2012)

B. Tincu et al., Investigation of plasma-assisted functionalization of pristine single layer graphene. Chem. Phys. Lett. **789**, 139330 (2022)

J. Toman et al., On the transition of reaction pathway during microwave plasma gas-phase synthesis of graphene nanosheets: from amorphous to highly crystalline structure. Plasma. Process. Polym. **18**, e2100008 (2021)

G.M. Tomboc, H. Kim, Derivation of both EDLC and pseudocapacitance characteristics based on synergistic mixture of NiCo2O4 and hollow carbon nanofiber: an efficient electrode towards high energy density supercapacitor. Electrochim. Acta **318**, 392–404 (2019)

P.S. Toth et al., Symmetric and asymmetric decoration of graphene: bimetal-graphene sandwiches. Adv. Func. Mater. **25**(19), 2899–2909 (2015)

D. Tsyganov et al., On the plasma-based growth of 'flowing' graphene sheets at atmospheric pressure conditions. Plasma Sources Sci. Technol. **25**(1), 015013 (2015)

D. Tsyganov et al., Microwave plasma-based direct synthesis of free-standing N-graphene. Phys. Chem. Chem. Phys. **22**(8), 4772–4787 (2020)

C.-H. Tu et al., Heteroepitaxial nucleation and growth of graphene nanowalls on silicon. Carbon **54**, 234–240 (2013)

Y. Tzeng et al., The synthesis of graphene nanowalls on a diamond film on a silicon substrate by direct-current plasma chemical vapor deposition. Carbon **53**, 120–129 (2013)

L. Van Nang, E.-T. Kim, Controllable synthesis of high-quality graphene using inductively-coupled plasma chemical vapor deposition. J. Electrochem. Soc. **159**(4), K93–K96 (2012)

R. Vitchev et al., Initial stages of few-layer graphene growth by microwave plasma-enhanced chemical vapour deposition. Nanotechnology **21**(9), 095602 (2010)

S. Vizireanu et al., Carbon nanowalls growth by radiofrequency plasma-beam-enhanced chemical vapor deposition. Plasma. Processes. Polym. **5**(3), 263–268 (2008)

I. Vlassiouk et al., Role of hydrogen in chemical vapor deposition growth of large single-crystal graphene. ACS Nano **5**(7), 6069–6076 (2011)

D. Vollath, Plasma synthesis of nanopowders. J. Nanopart. Res. **10**(1), 39–57 (2008)

S. Wagner et al., Noninvasive scanning Raman spectroscopy and tomography for graphene membrane characterization. Nano Lett. **17**(3), 1504–1511 (2017)

J. Wang et al., Synthesis of carbon nanosheets by inductively coupled radio-frequency plasma enhanced chemical vapor deposition. Carbon **42**(14), 2867–2872 (2004)

X. Wang, L. Zhi, K. Müllen, Transparent, conductive graphene electrodes for dye-sensitized solar cells. Nano Lett. **8**(1), 323–327 (2008)

Y. Wang et al., Supercapacitor devices based on graphene materials. J Phys. Chem C. **113**(30), 13103–13107 (2009)

S. Wang et al., Synthesis of graphene on a polycrystalline Co film by radio-frequency plasma-enhanced chemical vapour deposition. J. Phys. D Appl. Phys. **43**(45), 455402 (2010)

Z. Wang, M. Shoji, H. Ogata, Carbon nanosheets by microwave plasma enhanced chemical vapor deposition in CH4–Ar system. Appl. Surf. Sci. **257**(21), 9082–9085 (2011)

Z. Wang et al., Microwave plasma-assisted regeneration of carbon nanosheets with bi-and trilayer of graphene and their application to photovoltaic cells. Carbon **67**, 326–335 (2014)

B. Wang et al., Plasma effects in aligned carbon nanoflake growth by plasma-enhanced hot filament chemical vapor deposition. Appl. Surf. Sci. **325**, 251–257 (2015)

Z. Wang et al., Free radical sensors based on inner-cutting graphene field-effect transistors. Nat. Commun. **10**(1), 1–10 (2019)

J.-B. Wang et al., A review of graphene synthesisatlow temperatures by CVD methods. New. Carbon. Mater. **35**(3), 193–208 (2020)

J.K. Wassei et al., Chemical vapor deposition of graphene on copper from methane, ethane and propane: evidence for bilayer selectivity. Small **8**(9), 1415–1422 (2012)

W. Wei, X. Qu, Extraordinary physical properties of functionalized graphene. Small **8**(14), 2138–2151 (2012)

Y. Wei et al., The nature of strength enhancement and weakening by pentagon–heptagon defects in graphene. Nat. Mater. **11**(9), 759–763 (2012)

Y. Wei et al., Dry plasma synthesis of graphene oxide–Ag nanocomposites: a simple and green approach. Mater. Res. Bull. **53**, 145–150 (2014)

K.E. Whitener Jr., P.E. Sheehan, Graphene synthesis. Diam. Relat. Mater. **46**, 25–34 (2014)

Y. Wu et al., Carbon nanowalls and related materials. J. Mater. Chem. **14**(4), 469–477 (2004)

S. Wu et al., Ultrasensitive and stretchable strain sensors based on mazelike vertical graphene network. ACS Appl. Mater. Interfaces. **10**(42), 36312–36322 (2018)

S.-L. Wu et al., Synthesis of carbon nanotubes with controllable diameter by chemical vapor deposition of methane using Fe@ Al2O3 core–shell nanocomposites. Chem. Eng. Sci. **217**, 115541 (2020)

Z.-L. Xu, B. Zhang, J.-K. Kim, Electrospun carbon nanofiber anodes containing monodispersed Si nanoparticles and graphene oxide with exceptional high rate capacities. Nano Energy **6**, 27–35 (2014)

T. Yamada et al., Low-temperature graphene synthesis using microwave plasma CVD. J. Phys. D Appl. Phys. **46**(6), 063001 (2013)

W. Yang et al., Carbon nanomaterials in biosensors: should you use nanotubes or graphene? Angew. Chem. Int. Ed. **49**(12), 2114–2138 (2010)

W. Yang et al., Growth, characterization, and properties of nanographene. Small **8**(9), 1429–1435 (2012)

C. Yang et al., Direct PECVD growth of vertically erected graphene walls on dielectric substrates as excellent multifunctional electrodes. J. Mater. Chem a. **1**(3), 770–775 (2013)

J. Yang et al., Wearable temperature sensor based on graphene nanowalls. RSC Adv. **5**(32), 25609–25615 (2015)

J. Yang et al., Three-dimensional conformal graphene microstructure for flexible and highly sensitive electronic skin. Nanotechnology **28**(11), 115501 (2017)

J.-S. Yang, D.Z. Pai, W.-H. Chiang, Microplasma-enhanced synthesis of colloidal graphene quantum dots at ambient conditions. Carbon **153**, 315–319 (2019a)

J. Yang et al., Flexible, tunable, and ultrasensitive capacitive pressure sensor with microconformal graphene electrodes. ACS Appl. Mater. Interfaces. **11**(16), 14997–15006 (2019b)

K. Yi et al., A two-dimensional cross-linked polythiophene network. J. Mater. Chem C. **7**(30), 9362–9368 (2019)

K. Yu et al., Growth of carbon nanowalls at atmospheric pressure for one-step gas sensor fabrication. Nanoscale. Res. Lett. **6**(1), 1–9 (2011)

H. Yu et al., High-efficient synthesis of graphene oxide based on improved hummers method. Sci. Rep. **6**(1), 1–7 (2016)

G. Yuan et al., Graphene sheets via microwave chemical vapor deposition. Chem. Phys. Lett. **467**(4–6), 361–364 (2009)

M.A. Zafar, M.V. Jacob, Synthesis of free-standing graphene in atmospheric pressure microwave plasma for the oil-water separation application. Appl. Surf. Sci. Adv. **11**, 100312 (2022)

M.A. Zafar et al., Single-step synthesis of nitrogen-doped graphene oxide from aniline at ambient conditions. ACS Appl. Mater. Interfaces **14**, 5797–5806 (2022)

M.A. Zafar et al., Electrochemical sensing of oxalic acid using silver nanoparticles loaded nitrogen-doped graphene oxide. Carbon Trends **8**, 100188 (2022a)

M.A. Zafar et al., Single-step synthesis of nitrogen-doped graphene oxide from aniline at ambient conditions. ACS Appl. Mater. Interfaces. **14**(4), 5797–5806 (2022b)

Z. Zhai et al., Metal-free synthesis of boron-doped graphene glass by hot-filament chemical vapor deposition for wave energy harvesting. ACS Appl. Mater. Interfaces. **12**(2), 2805–2815 (2020)

M. Zhang, J. Li, Carbon nanotube in different shapes. Mater. Today **12**(6), 12–18 (2009)

B. Zhang et al., Low-temperature chemical vapor deposition growth of graphene from toluene on electropolished copper foils. ACS Nano **6**(3), 2471–2476 (2012)

L. Zhang et al., Understanding the growth mechanism of vertically aligned graphene and control of its wettability. Carbon **103**, 339–345 (2016)

W. Zheng, X. Zhao, W. Fu, Review of vertical graphene and its applications. ACS Appl. Mater. Interfaces. **13**(8), 9561–9579 (2021)

J. Zhou et al., Ferromagnetism in semihydrogenated graphene sheet. Nano Lett. **9**(11), 3867–3870 (2009)

Q.-L. Zhu, Q. Xu, Immobilization of ultrafine metal nanoparticles to high-surface-area materials and their catalytic applications. Chem **1**(2), 220–245 (2016)

M. Zhu et al., A mechanism for carbon nanosheet formation. Carbon **45**(11), 2229–2234 (2007)

Y. Zhu et al., Carbon-based supercapacitors produced by activation of graphene. Science **332**(6037), 1537–1541 (2011)